



University of
Nottingham

UK | CHINA | MALAYSIA

**An operational platform towards
accelerating wound healing through
electrical stimulation and drug delivery,
with the collection of analytes**

By Zijian LI

Supervisors Prof. Xu Sun

Dr. Sheng Zhang

A master thesis submitted for the degree of Master
of Mechanical Engineering of Nottingham
University

Department of Mechanical, Materials, and
Manufacturing Engineering

August 2024

(This page is left blank)

Abstract

The skin acts as the most significant barrier against external infections, and the healing process of the skin is highly complex and vital. Chronic wounds not only heal slowly but can also cause a range of serious complications that can lead to life-threatening consequences. Billions of dollars have been invested in researching ways to accelerate wound healing. Traditional wound dressings only function to prevent outer infection, but they have many limitations and do not accelerate wound healing. Electrical stimulation (ES) has been demonstrated to accelerate tissue growth and cell migration. Therefore, recent studies have integrated ES with wound dressings.

Other factors, for instance, drug delivery and breathability, were also essential for wound recovery in addition to ES. Therefore, a breathable smart wound dressing has been designed in this work. This wound dressing serves as a platform that can provide ES, deliver medicine to the wound, and collect the wound exudates as analytes for glucose levels.

To accomplish these functions, the wound dressing in this project was designed from the following aspects.

(i) **Liquid delivery and breathability:** Polydimethylsiloxane (PDMS) has superb biocompatibility and hydrophobicity, making it an ideal wound dressing. However, PDMS cannot allow liquid to pass through, which hinders the transportation of oxygen and blood to the wound. In this study, unidirectional channels were designed to facilitate the delivery of blood and air. Additionally, wound dressing enables the delivery of medicine to the wound. The optimal channel size has been simulated using the finite element analysis software COMSOL. Additionally, the unidirectional liquid delivery ability has also been tested using a contact angle test machine.

(ii) **Conductive and mechanical performance:** As an insulating material, PDMS needs to be supplemented with additional conductive materials in PDMS-based wound dressings to equip conductivity. Silver has excellent conductivity, and in addition, Ag ions can act on bacteria through a variety of mechanisms, including binding to proteins in the bacteria, damaging the cell structure of the bacteria, and causing the bacteria to

die. In this work, silver paste was used to decorate the wound dressing. The shape of silver traces was determined by simulation using COMSOL. Additionally, the performance of silver traces combined with a PDMS base was also simulated using COMSOL. The conductive performance of this wound dressing was recorded under deformation using a stretching machine and a resistance tester.

(iii) **Flexible and wearable battery:** Although there are many nanogenerators, most commercial wound dressings with ES still use batteries as a power supply source. This is because these nanogenerators have many limitations, including low power density, unstable power supply, and high cost. In this work, a 6.2mm diameter button cell was selected as the power source. The button cell was encapsulated by PDMS, and carbon paper was cut to serve as the conductive electrode.

(iv) **Glucose detection:** Blood is an ideal analyte because it contains a wealth of biological information that can reflect the health of the human body. And in the initial wound healing process, there will generate lots of blood from the wound. The wound dressing proposed in this work is mainly used in chronic wounds, for example diabetic wounds. Thus, a blood reservoir was fabricated to collect and analyze the glucose level.

Acknowledgements

As I conclude this thesis, I am overwhelmed with gratitude towards all those who have generously contributed to my graduate studies and the development of this dissertation. First and foremost, I would like to express my profound appreciation to my supervisor, Professor Xu Sun. Professor Sun has provided invaluable insights and advice throughout my research journey, offering fresh perspectives that enriched my study. At crucial junctures, her timely guidance illuminated complex issues, enabling me to proceed smoothly. Her rigorous academic standards and unwavering dedication to her students have left a profound impression on me. I am sincerely grateful to Professor Sun for her contributions.

Furthermore, I must extend my heartfelt thanks to Professor Sheng Zhang. With his vast knowledge, rigorous academic approach, and keen insight, Professor Zhang has guided me throughout the process of selecting my research topic, constructing the framework, writing the content, and refining the final draft. Whenever I encountered obstacles or uncertainties, he patiently listened and, with his profound expertise and extensive experience, illuminated the path forward. Professor Zhang has not only taught me how to conduct research but also, through his exemplary character, imparted valuable lessons about responsibility and commitment. I am deeply indebted to him for his unwavering support and guidance.

Lastly, I am deeply thankful to my family. Your unconditional love and steadfast support have been my rock throughout. When faced with challenges and difficulties, your encouragement has reinvigorated my spirit and propelled me forward. This gratitude is something I will forever cherish in my heart.

Once again, I express my sincerest thanks to everyone who has contributed to my graduate studies and the completion of this dissertation. Your contributions have been invaluable and have fueled my progress.

Publications

Papers under review

Zijian LI, Chen Liu, Qianqian Wang, Zhaotao He, Sheng Zhang, Xu Sun. Functional materials applied to self-powered smart skins towards wound management[J]. Advanced Materials Technologies, Under review, 2024.5.27.

Content

1. Introduction.....	1
1.1 Background.....	1
1.2 The stage of wound healing	4
1.3 The principle of ES	5
1.3.1 Endogenous electric field of skin wounds.....	6
1.3.2 Exogenous electrical stimulation for skin wound healing.....	6
1.3.3 The working principle of ES on wound healing.....	7
1.4 Wound exudate.....	8
1.5 Conclusion	9
1.6 Novelty.....	10
2. Literature review	11
2.1 Introduction.....	11
2.2 Liquid management.....	11
2.2.1 Textiles	12
2.2.2 Microfluid channels	14
2.3 Conductive wound dressings.....	16
2.3.1 Film.....	17
2.3.2 Membrane	18
2.3.3 Hydrogel.....	18
2.3.4 Liquid conductive materials.....	19
2.4 Wound dressings with ES.....	21
2.4.1 TENGs	21
2.4.2 PENGs.....	23
2.4.3 EBFC.....	25
2.4.4 Built-in batteries.....	27
2.5 Conclusion	28
3. Methods and materials	31
3.1 Liquid delivery	31
3.1.1 Finite element analysis.....	32
3.1.2 Unidirectional liquid delivery	32
3.1.3 Drug delivery	33
3.2 Mechanical and conductive performance.....	34
3.2.1 Finite element analysis of mechanical performance	34
3.2.2 Conductive performance	35

3.3 Flexible and wearable battery module	36
3.4 Glucose detection.....	36
3.5 Construction of PBWDP.....	38
4. Results and Discussion.....	40
4.1 Liquid delivery.....	40
4.1.1 The principle of microfluid	40
4.1.2 Finite element analysis.....	41
4.1.3 Unidirectional liquid delivery	43
4.1.4 Drug delivery	45
4.2 Mechanical and conductive performance.....	47
4.2.1 Finite element analysis of mechanical performance	47
4.2.2 Conductive properties	51
4.3 Flexible and wearable battery module	53
4.4 Glucose detection.....	55
5. Conclusion	58
6. Dissicussion	59
Reference	61

1. Introduction

1.1 Background

The skin, the largest organ of the human body, plays a significant role in daily human activities by detecting the external environment and preventing bacteria and pathogens.^{1, 2} Owing to its elastic and soft skin properties, it is prone to generating defects and injuries, referred to as wounds.^{3, 4} When a wound occurs, the skin can repair itself. However, the skin is no longer a barrier against bacteria and pathogens during this period. Additionally, proper wound care is necessary during the healing process to protect against contamination, alleviate pain, accelerate wound healing time, and prevent scar formation.⁵ However, some injuries exhibit impaired healing processes that fail to proceed in a timely and coordinated manner. The expense of treating skin injuries is on the rise every year, impacting millions of individuals globally. Consequently, the wound healing process, which aims to return the affected area to its normal state, is crucial and time-sensitive. As our understanding of the healing process continues to grow, there has been a shift in focus towards more intricate microenvironment therapy for chronic wounds, moving away from simple debridement and topical dressing.

One well-known fact is that diabetes has one of the most critical impacts on human health. Not only does it cause organ disease, but it also hinders wound healing and can even lead to amputation.^{6, 7} The precise coordination and integration of complex biological and molecular processes, including cell migration, proliferation, extracellular matrix deposition, and angiogenesis, are necessary for normal wound healing.⁸ However, people with diabetes with high glucose levels create a complicated wound environment, such as tissue hypoxia and difficulty recovering from hyperglycemia. In addition, diabetic wounds are vulnerable to pathogenic bacteria due to the compromised immune system of diabetic patients.⁹ High glucose level makes them more susceptible to infections and slower healing processes. Therefore, it is

crucial to manage the wound carefully.

During wound healing, oxygen is essential for promoting cell migration and proliferation.¹⁰ Oxygen also plays a crucial role in facilitating cell energy production, which is necessary for their movement and division during healing. Additionally, oxygen helps regulate inflammation and support immune function at the injury site, aiding in the repair and regeneration of damaged tissue. Without sufficient oxygen from the air, compromised wound healing may lead to delayed or impaired recovery. Unlike dry wound treatment, moist or wet wound therapies have demonstrated efficacy in enhancing re-epithelialization and minimizing scar formation.¹¹ In a moist or dry recovery environment, the inflammatory response is mitigated, thus constraining the advancement of injury. In addition to the recovery environment, an essential quality of our skin is its ability to conduct electricity, which holds significant importance in a range of human endeavors.¹²

Recent research finds that electrical stimulation (ES) could accelerate wound healing, as the skin generates electric fields ranging from 40-200mV/mm to restore the wound.¹³⁻¹⁵ A wound healing patch made of a conductive material, possessing conductivity similar to the skin's, demonstrates significant potential in promoting wound healing, particularly for challenging cases such as full-thickness acute wounds, infected wounds, and diabetic wounds, which are difficult to recover.^{16, 17} Nerve regeneration represents a complex phase within the wound healing process.¹⁸ Consequently, wound therapy endeavors to expedite the healing duration, foster nerve regeneration, and reinstate excitation functions.¹⁹ Besides, during the wound recovery process, there are still many factors that need to be considered, such as oxygen levels,²⁰ hyperglycemia,⁷ excessive reactive oxygen species (ROS),²¹ and so on.

Procellera dressing is a commercially ES wireless device for wound healing.²² The power supply module was made of silver/zinc arrays and thin polyester cloth, which cannot generate ES for a long time due to the consumption of silver/zinc arrays and the poor moisturizing ability of polyester cloth. Yu et al. used a medical cotton cushion as the substrate, the medical cotton cushion could absorb much water and keep wet for an extended time.²³ In this work, a biocompatible agglomerate was chosen to create a

slurry containing AgNPs and ZnNPs, which was subsequently applied onto one side of the medical cotton cushion using a dot matrix-arrayed technique at a thickness of 2 mm. This Ag/Zn patch is moistened with sterile saline solution or water and then applied to the wound.

However, this ES generation method is not convenient for wound healing. The softness and elasticity of human skin pose a challenge for metal patches to adapt thoroughly. This phenomenon is due to the significant difference in Young's modulus between metal materials and the skin. The dynamic nature of our bodies, including constant movement and activities like breathing, leads to changes in the position and shape of body parts. Consequently, metal patches may result in detachment and displacement, hindering optimal wound healing. Therefore, in the next several years, few studies have been conducted on this method.

In addition to the factors mentioned above, applying medication to the wound is widely recognized as an effective method for expediting wound healing. This approach entails using diverse topical ointments, creams, and gels specifically formulated to stimulate tissue regeneration and mitigate the risk of infection. These pharmaceuticals often incorporate components such as antibiotics, antiseptics, and growth factors that can facilitate the body's innate healing processes. Moreover, administering medication to a wound can also afford pain relief and alleviate discomfort associated with the injury. Many topical treatments possess analgesic properties capable of numbing the affected area and reducing inflammation, enhancing patient comfort throughout the healing process.

Therefore, it is crucial to emphasize the importance of meticulous wound management throughout wound healing. Many wound healing methods have been developed, including negative-pressure therapy, hyperbaric oxygen therapy, electrotherapy, and topical drug and growth factor delivery. However, regardless of the healing process used, wound dressings are necessary. Traditional dressings such as medical tapes and bandages do little to accelerate wound healing. Additionally, traditional wound dressings adhere to the wound, which is not conducive to tissue growth; therefore, replacing traditional wound dressings may cause secondary injury to

the wound.

According to this, researchers have begun to integrate functions including wound exudates management, antimicrobial properties, drug delivery, and ES into wound dressings. These smart wound dressings not only manage the wound environment by controlling the amount of exudate but also prevent infections, promote faster healing by releasing therapeutic agents, and can even assist in tissue regeneration through the application of ES that demonstrated great potential in the wound healing.

1.2 The stage of wound healing

The wound healing process can be divided into four phases: the coagulation phase, the inflammation phase, the proliferation phase, and the remodeling phase.²⁴ Some chronic wounds are difficult to heal solely through the body's own repair mechanisms; for instance, diabetes causes high levels of glucose that disturb the microenvironment and interfere with the repair process.²⁵

The phase of hemostasis and inflammation is a critical stage that immediately follows tissue injury. Hemostasis involves the formation of a clot to stop bleeding, which includes platelet activation and the coagulation cascade.²⁶ This leads to the formation of a plug at the injury site, as well as the conversion of soluble fibrinogen into insoluble fibrin strands to stabilize the platelet plug. Key molecules released during this stage include cytokines, which regulate the immune response, and growth factors that promote cell proliferation and tissue repair. Inflammation also assists in removing bacteria and foreign bodies from the wound to prevent infection.

During the proliferation stage, neovascularization develops, and cells undergo multiplication and differentiation to facilitate tissue repair. The newly formed capillaries extend into the wound site, delivering oxygen and nutrients to support cellular growth and specialization. Cellular proliferation entails the recruitment of neighboring tissue cells to the wound site, including fibroblasts responsible for collagen production and extracellular matrix components, keratinocytes contributing to epidermal formation, and endothelial cells lining the nascent blood vessels. Fibroblasts

play a pivotal role in this stage by not only synthesizing collagen for structural integrity but also releasing growth factors to promote further cellular proliferation and differentiation.

The remodeling stage is the final phase of the wound healing process, where the newly formed tissue undergoes maturation and restructuring to regain its strength and function. This process also involves reducing blood vessel density and the transformation of fibroblasts into myofibroblasts to facilitate wound contraction. Matrix metalloproteinases play a pivotal role in regulating ECM synthesis and degradation during this phase, ultimately leading to functional recovery and scar maturation.

In conclusion, it is crucial to consider factors including managing wound exudates, preventing bacterial infection, and promoting expedited recovery throughout the process of wound healing.

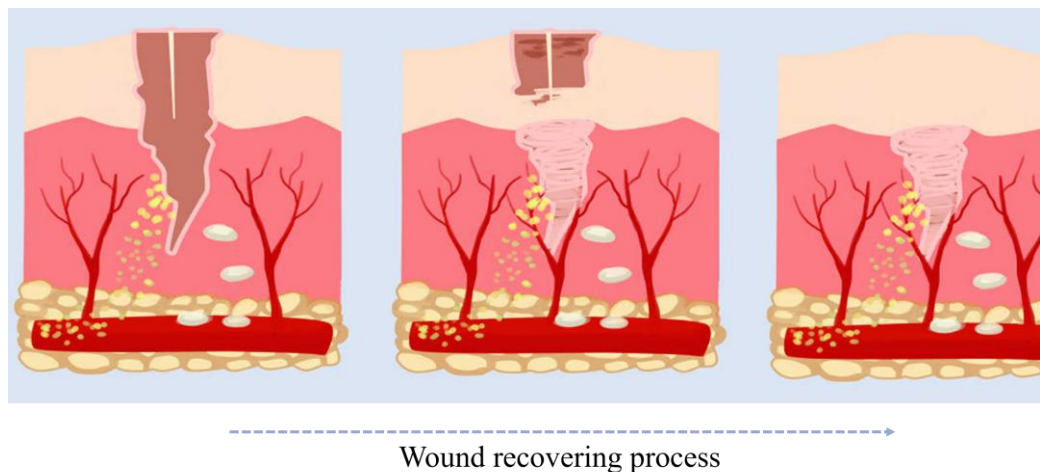


Figure 1.1 Tissue remodeling process

1.3 The principle of ES

Ever since the initial observation of endogenous current in wounds by German physiologist Emil Du-Bois Reymond, researchers have identified bioelectricity in the wounds of different animal species.²⁷ Various studies have been carried out on the existence of bioelectricity and its potential to accelerate wound healing. Afterward, some research has demonstrated that bioelectricity can enhance the speed of wound

healing by promoting the movement of essential cells.

1.3.1 Endogenous electric field of skin wounds

Several years ago, Barker et al. first proposed the concept of the "skin battery" theory, suggesting a negative relationship between electric field intensity and the distance from the wound edge.²⁸ Ghadamali et al. found that the endogenous electric field of acute skin is associated with the size of the wound surface.²⁹ The directional transport of ions by polarized epithelial cells has been demonstrated to be related to the generation of endogenous electric fields on skin wounds. The current across the cell is generated by the asymmetric distribution between the Na^+ and Cl^- channel, located in the apical plasma membrane, and the K^+ and Cl^- channel, on the basal plasma membrane. Due to the difference in electric potential between the injured area, which functions as a cathode, and the healthy skin surrounding the wound, there is a low-level flow of direct current from the healthy skin to the wound. In addition, researchers manipulated the number of ion pumps to change the intensity of wound potential and found that the variation in wound potential influences the speed of wound recovery.

1.3.2 Exogenous electrical stimulation for skin wound healing

Since the 1960s, researchers have been investigating the impact of electrical stimulation therapy on wound healing. Exogenous ES is primarily used in wound treatment to mimic wound potential. ES can induce the movement of charged ions through epidermal ion channels to direct the migration of dermal cells (including keratinocytes, endothelial cells, and fibroblasts) at the wound edge towards the center, as shown in Fig.1.2.³⁰ The process of ES also contributes to an augmented secretion of biomolecules, including transforming growth factor (TGF), vascular endothelial growth factor (VEGF), fibroblast growth factor (FGF), and epidermal growth factor (EGF).³¹ Those factors have functions of speed up the blood vessel formation, nerve repair and the tissues recovery. The ES not only accelerate the speed of wound healing but also avoid the bacteria infection. In addition, the ES could regulate cell activity and

promoting the secretion of growth factors which will reduce the scars formation.

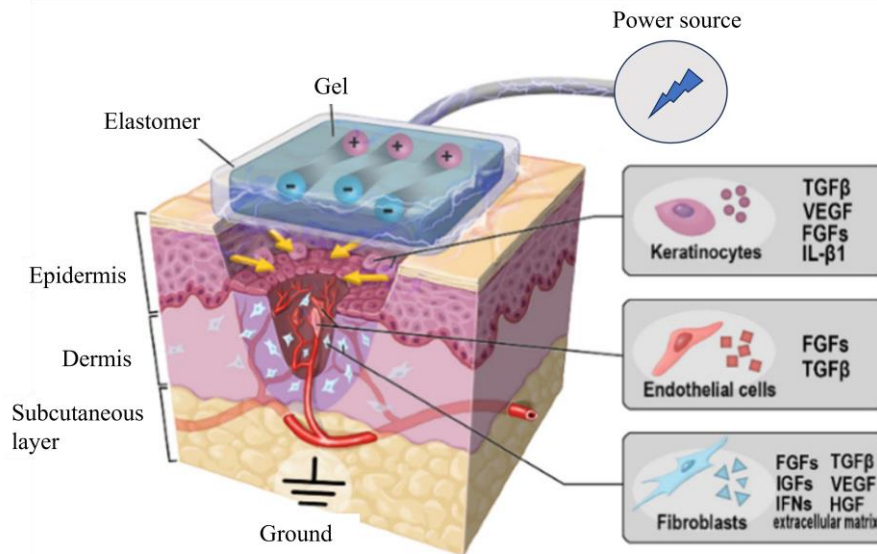


Figure 1.2 The organism of ES to accelerate wound healing³⁰

1.3.3 The working principle of ES on wound healing

The ES could accelerate the recruitment of immunocytes and enhance the antibacterial property of patches.³² During the early phase of inflammation, accelerating the recruitment of immune cells and cytokines promotes wound healing. The macrophages, lymphocytes, and neutrophils can migrate to the wound driven by endogenous electrical stimulation. Once those factors arrived at the wound, these immune cells work together to clear away debris, fight off infection, and promote healing. ES can reduce the number of immune cells and cytokines in the late phase of inflammation, which plays a certain role in resolving inflammation. When the bacterial concentration reaches a specific threshold, the inflammatory cells become ineffective in eliminating these microorganisms.

Additionally, long-term use of antibiotics for chronic wounds also fails due to antibiotic resistance. Wolcott et al. conducted groundbreaking research on the impact of external ES on the antibacterial properties in living organisms.³³ They applied negative polarity direct current to address chronic wounds infected with *Pseudomonas* and *Proteus* species and observed that the chronic wound was pathogen-free a few days later.

The ES could enhance tissue growth and cell migration and proliferation. ES has been applied as an assisting method to increase tissue blood flow. With the increased blood flow, more nutrients could be delivered to the wound area. In addition, in the study by Zeniab Khalil et al., they found that low-frequency ES can activate vascular response in aging rats.³⁴ Jin et al. discovered that improved vasodilation, increasing blood flow, could potentially enhance the effectiveness of electrical stimulation on wound healing.³⁵ Research has indicated that electrical stimulation therapy can be advantageous in promoting tissue blood circulation and expediting the process of wound recovery. In addition, abundant studies have proven that the ES could control cell-directed migration to accelerate tissue formation and epithelium. Alvarez et al. and Mertz et al. discovered that applying anodic DC and high voltage pulsed current (HVPC) electrical stimulation accelerated the epidermis formation.³⁶ Konstantinos et al. reported a notable augmentation in scratch closure and proliferation rates following electrical stimulation.³⁷

During the remodeling stage, the ES could also reduce the formation of scars. At this stage, a significant amount of collagen accumulates, closely associated with scar tissue formation. Habiba et al. conducted a study using low-voltage pulsed current (LVPC) electrical stimulation to investigate the potential mechanism of wound closure in diabetic mice.³⁸ Their findings indicated a positive correlation between collagen deposition in deep scars and the intensity of electrical stimulation. The results suggested that electrical stimulation could potentially impact the tensile strength of scars.

1.4 Wound exudate

The wound exudate is an inevitable question during the wound healing process.³⁹ In the initial stage, the wound exudate is mainly blood. The wound exudate also generates in the inflammation phase of the acute wound. However, for chronic wounds (e.g. diabetic wound) always generate high level wound exudate since they without abnormal inflammation markers that present in acute wounds.

The wound exudate management is also vital important to the wound healing. Poor

exudate management will extend time period of wound healing process and may add the risk of bacterial infection. Since the wound will under dehydration under the less exudate environment that leads to the wound dressing adhere to tissues. The wound will suffer damage again when remove the wound dressing. However, if the wound under a over moist environment, the skin is prone to breakdown since the maceration and hinder the cell migration.

Thus, a superb wound dressing should equip the ability of wound exudate management. The moist environment could accelerate wound healing by optimally regulating oxygen tension, essential for cellular respiration and metabolism. In addition, the moist environment facilitates vascular growth, ensuring nutrient and oxygen supply, and waste removal.

1.5 Conclusion

Thus, in this work, we developed a conductive PDMS-based wound dressing platform (PBWDP) that can fulfill the functions outlined in the conclusion.

(i) Superb mechanical and electrical performance

The PDMS has a Young's modulus similar to skin that offers exceptional biocompatibility and flexibility. In addition, the PBWDP equip special mechanical design to enhance its mechanical performance. At the side of the patch near the skin, we created a path with silver traces, which can help balance the electrical field around the wound, and Ag^+ could kill bacteria. Additionally, it can be connected to external power sources to generate ES. This smart wound dressing serves as a platform that enables users or doctors to directly operate the wound (e.g., clean the wound, change medicine or ES) on the dressing during any different tissue remodeling period. In this study, the PBWDP showed great potential in wound healing, extends the application range of wound management, and provides a new therapeutic solution to promote nerve recovery and anti-bacteria.

(ii) Wound exudate management

The substrate is fabricated using PDMS due to its excellent hydrophobicity,

biocompatibility, and flexibility, making it easy to remove and wear. For the absorbent ability of hydrogels, we designed unidirectional channels inside the PDMS substrate that allow blood to flow out of the patch and drugs to flow into the patch respectively through capillary force. In addition, the away skin side of PBWDP is waterproof and is set as a barrier to prevent outer infection.

(iii) Other functions

To ensure the PBWDP has a stable ES, a flexible battery was constructed with a button cell with small size, PDMS and carbon cloth. In addition, a drug delivery layer was fabricated with silica gel that could enhance the drug delivery efficiency and reduce uncomfortable feelings. The blood could be collected by the blood reservoir during wound recovery to detect glucose levels.

1.6 Novelty

(1) Excellent biocompatibility and simplified fabrication process: The PBWDP used PDMS as the base and designed special channels to enhance breathability and manage wound exudates. PDMS has excellent biocompatibility and a convenient preparation method. Other materials, such as hydrogels and piezoelectric fibers, are complicated to fabricate, and some of them are toxic, posing potential risks to patients' health. PDMS is also known for its flexibility and durability, making it an ideal material for medical devices requiring repeated use.

(2) Multifunctional platform: Instead of other wound dressings, the PBWDP provides an operational platform where users can handle wounds without removing the dressing. In addition, the wound exudates could be collected to analyze the glucose level.

2. Literature review

2.1 Introduction

There are three crucial aspects in designing a smart wound dressing. The first and most significant one is liquid management as the wound will produce liquid, including blood and interstitial fluid, and failure to promptly remove the wound exudates will impede wound recovery. The secondary aspect is the conductive property. The skin has been demonstrated to have conductivity, but there are still many challenges in constructing a flexible and conductive wound dressing. The final aspect is the electrical stimulation. A successful wound dressing should be convenient, and thus the self-powered devices were discussed. Since the wound dressing is a kind of wearable device and the development of wearable devices is outpacing that of wound dressings, in this work, wearable devices were also discussed. When designing a smart wound dressing, the first issue to be addressed is the ability to manage liquid as excessive accumulation of wound exudates hinders the recovery process. Conductive wound dressings have been shown to accelerate wound healing. Additionally, ES can promote cell migration and proliferation and kill bacteria. Therefore, in this work, three topics were discussed, respectively: fluid management, conductive wound dressings, and ES wound dressings.

2.2 Liquid management

The breathability and fluid transport capacity of wound dressings are critical considerations in the management of wounds.⁴⁰ Proper breathability allows oxygen to reach the wound, promoting healing, while effective fluid transport helps prevent the build-up of excess moisture, which can lead to infection. These factors also affect patient comfort and overall wound care efficiency. Therefore, selecting the right dressing with optimal breathability and fluid transport capacity is essential for successful wound treatment. Nowadays, wearable electronics are emerging as a trend for motion detection, health monitoring, and interpersonal interaction. However,

transporting human exudates, including sweat and blood, remains a major challenge. Therefore, there has been a significant amount of research on the issue of fluid accumulation that could also serve as inspiration for the design of wound dressings.

2.2.1 Textiles

Textiles with high breathability are designed to allow air and water vapor to easily pass through the fabric, creating a more comfortable experience for the wearer. Furthermore, the textile patch could be securely adhered to the surface of the skin.

Bandages, cotton, rayon and other materials were mainly used to fabricate traditional wound dressings. These materials are only suitable for dry and clean wounds. Electrospinning could quickly generate the ultrathin fibers that could make textile wound dressings.⁴¹ Wang et al. proposed an innovative self-propelling bandage, which represents a significant advancement in wound dressings. The use of electrospun hydrophobic nanofibers on hydrophilic gauze allows for the efficient removal of excess bodily fluids from injuries, promoting faster healing and reducing the risk of infection. Hu et al. proposed a Janus fiber dressing via electrospinning, which was made of well-aligned Ag nanoparticles (AgNPs) and nanofibers of polycaprolactone/gelatin (PCL/Gel), as shown in Fig.2.1a.²⁵ The Janus dressing can not only drain excess fluid from the wound, but also the AgNPs enable the dressing to have anti-bacterial properties. Yang et al. used electrospinning to fabricate a Janus wound dressing, using polyvinylpyrrolidone (PVP) and ethyl cellulose (EC) polymer matrices to create the textile base.⁴² In this work, AgNPs were incorporated into the electrospinning process, and ciprofloxacin was also loaded to enhance the antibacterial performance.

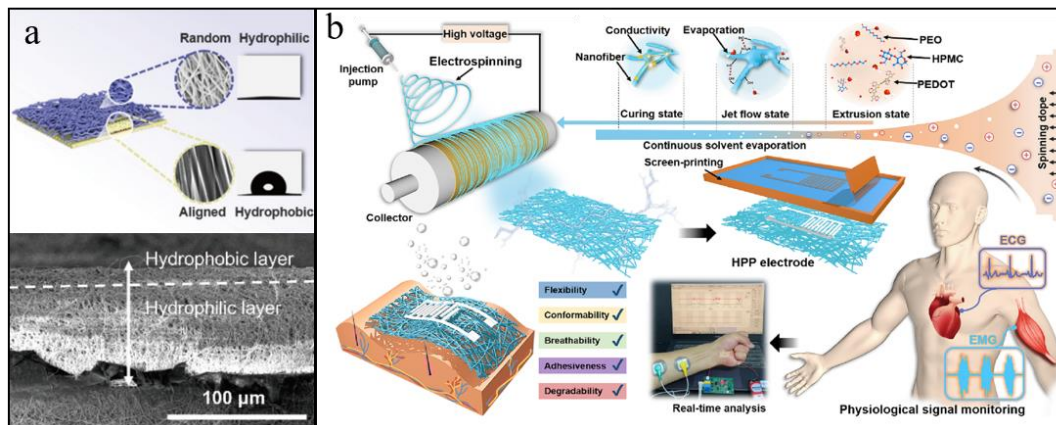


Figure 2.1 The textile patches(a. Ultrathin, flexible, and piezoelectric Janus patch; b Compliant and breathable patch)

For the wearable devices, Ma et al. developed a breathable epidermal electrode for electrophysiological monitoring, fabricated using the electrospinning method.⁴³ The skin-friendly materials hydroxypropyl methylcellulose (HPMC), polyethylene oxide (PEO), and poly (3, 4-ethylenedioxythiophene): polystyrene sulfonate (PEDOT: PSS) were mixed to obtain the electrospun fibers. Ma et al. utilized the electrospinning technique to fabricate porous fiber films using styrene-butadiene-styrene block copolymer (SBS).⁴⁴ This method created a highly interconnected network of fibers, resulting in a large surface area and high porosity. The HPMC exhibits a high water-vapor transmission rate of over $102 \text{ g} \cdot \text{m}^{-2} \text{ h}^{-1}$ at 37°C . Zheng et al. used the Polyurethane (PU) film to fabricate an ultrathin and breathable electronic tattoo (e-tattoo) for electrophysiological sensing.⁴⁵ The e-tattoo in this work was obtained through rod-coating, and the thickness could be controlled by changing the specifications of coating rods. The method of rod-coating enabled the PU film to have a porous structure, which enhanced its breathability. Luo et al. also used PU film to create the glucose-sensing patch.⁴⁶ However, this sensor patch was fabricated by electrospinning the PU fibers, which have excellent stretchability and a porous structure that enables stability and sweat transmission ability during wearing. Yao et al. developed a breathable nanofibrous wound dressing using electrospun materials, including polyvinyl butyral (PVB)-PDMS and gelatin. The upper layer was comprised of PVB-PDMS, the middle layer consisted of PVB-PDMS/gelatin, and the lower layer was made of gelatin. Each

layer was designed with specific fiber distributions to create an asymmetric wettability gradient in the film. This dressing demonstrated excellent waterproofing and unidirectional liquid delivery capabilities.

2.2.2 Microfluid channels

The microfluidics technique has demonstrated superb performance in particle filtering and transferring. The specific microfluidic structure could also allow the liquid to flow in a specific direction. Thus, we introduced certain unique channel configurations.

Paper-based microfluidics could serve as a detection platform for bacteria and viruses, showing great potential in testing for severe acute respiratory syndrome, Ebola, and COVID-19. However, slow driving speed, low selectivity, and material constraints hinder long-term wear applications.

Therefore, the treatment and construction of 3D structures in other materials, such as PDMS, will become the future focus of development. Xu et al. construct PDMS film with laser micro drilling holes, and the hydrophilicity has been modified.⁴⁷ The wound dressing consists of PDMS Janus film as the primary dressing, filter paper as the absorbent layer, and medical adhesive tape as the secondary dressing. However, the therapeutic efficacy of these reported Janus wound dressings is limited by their single functionality. Wang et al. developed a novel sandwich-structured superlyophobic (SLO) dressing by integrating a PDMS layer and a gauze layer.⁴⁸ The PDMS was positioned beneath the gauze layer, and the PDMS layer was not a single piece but rather composed of multiple small pieces. Small gaps existed between the different PDMS pieces, serving as unidirectional channels for absorbing wound exudate. Ge et al. developed a smart wound dressing with wireless exudate management capabilities, integrating sensors, wound care, and flexible circuit modules.⁴⁹ The spiral microchannels embedded in the PDMS layer establish a sophisticated network for controlling wound exudate, engineered to effectively absorb and eliminate the exudate through micro-scale forces.

Additionally, there were many applications of special structural designed PDMS that could inspire novel wound dressings. Wang et al. introduced a water evaporation device with vertically ordered channels, as shown in Fig.2.2a.⁵⁰ This water evaporation device was inspired by the long-range ordered structure and water transport capacity of lotus stems. In the fabricating process, the ultra-long hydroxyapatite (HAP) nanowires act as heat-insulating skeletons. At the same time, polyacrylamide (PAM) and polyvinyl alcohol (PVA) are used as reagents to lower the water evaporation enthalpy and as glue to enhance the mechanical properties.

Mao et al. developed a swimming robot driven by Marangoni propulsion.⁵¹ This work obtained the microfluid channels by laser treatment on the PDMS. Additionally, water resistance was significantly reduced after laser treatment on the device's surface. The special microfluid channel design allowed the alcohol and air release in the sequence, as shown in Fig.2.2b. Finally, the chemical Marangoni propulsion phenomena will push the device to swim in route planning. Zhang et al. designed a bio-inspired nanofiltration channel through which the droplet could self-drive into the hole.⁵² The principle of droplet motion, as shown in Fig.2.1c, is driven by the anisotropic structure of spindle knots, which generates different surface tensions and causes the droplet to move. A similar structure has been shown in the research by Guo et al., as shown in Fig.2.2d.⁵³ Nepenthes inspired them and developed an underwater superoleophilic two-dimensional surface, which can transport droplets unidirectionally over long distances. The droplet could move from a high curvature to a low curvature on a shape-gradient surface. In this work, the surface was treated with superhydrophobic spray coating and laser etching. The schematic diagram and working method are shown in Fig.2.1e. Hsu et al. were inspired by the periodic spindle nodes in spider silk and conical barbs in cacti to construct a unidirectional wetting surface.⁵⁴ This study involved fabricating specific patterns using 3D printing technology and treating them with plasma and liquid chemical deposition. The multi-gradient surface is sufficient for manipulating the droplet to resist gravitational diffusion at different tilt angles, as shown in Fig.2.2f.

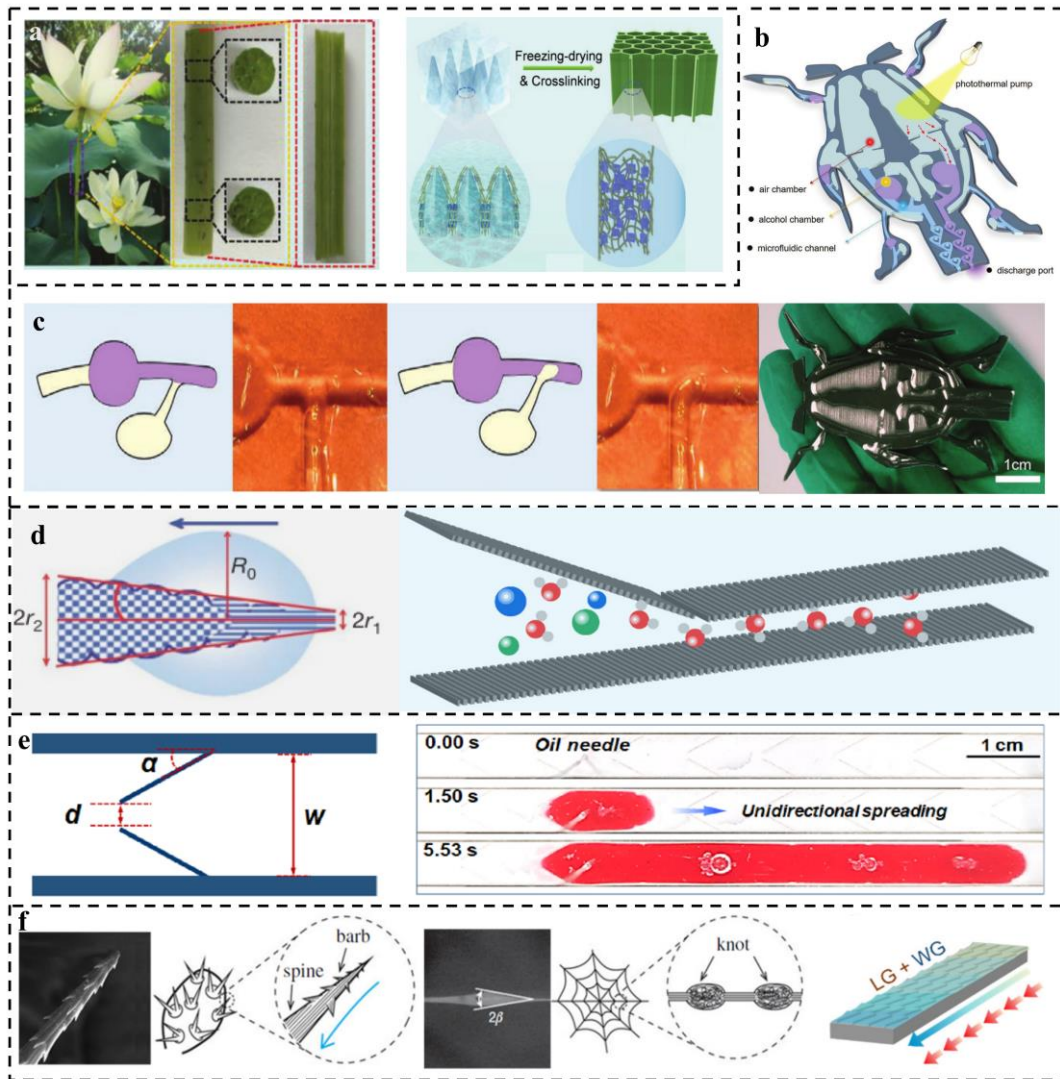


Figure 2.2 Specific design of microfluidic channel

2.3 Conductive wound dressings

Conductive materials have been found to possess conductivity similar to that of human skin. This characteristic allows them to effectively promote tissue regeneration and accelerate wound healing.⁵⁵ By creating an environment conducive to cell proliferation and migration, these materials show great potential in improving the outcomes of wound care treatments. Additionally, conductive materials also can manage bacterial growth and reduce infection risk, further enhancing their value in medical applications.

2.3.1 Film

The film, with thin size and semipermeable properties allowing the delivery of oxygen and water vapor, has been widely employed as wound dressings with added conductive materials to activate cell migration. Justin et al. used the polypyrrole film as the base to fabricate a controlled drug delivery system for wound healing. Since PPy can respond to electrical signals, the drug will be released from the PPy film when the drug control system receives the electrical signals, as shown in Fig.2.3a.⁵⁶ Marzocchi et al. coated poly(3,4-ethylenedioxythiophene) (PEDOT) on a commercial film to demonstrate its ability to enhance cell proliferation. In this study, the PEDOT was deposited on the film by spin coating and electrochemical polymerization. The results showed that the PEDOT film enhanced the growth of T98G cells, as shown in Fig.2.3b.⁵⁷ Pramanik et al. presented a polyaniline (PANI)-based film as a drug reservoir. In this work, the medicine curcumin was entrapped by PANI to promote tissue growth. However, PANI would degrade in vivo and could be cytotoxic to cells.¹ Simmons et al. developed a polyvinylpyrrolidone-iodine film decorated with carbon nanotubes (CNT) that has antibacterial properties, superb flexibility, oxygen permeability, and conductivity ($10 \text{ k}\Omega \text{ sq}^{-1}$).⁵⁸ However, the toxicity of CNT depends on many factors, including its length, diameter, impurities, and modified agents. Thus, considerable consideration needs to be taken when applying CNTs as conductive materials for wound dressings.⁵⁹

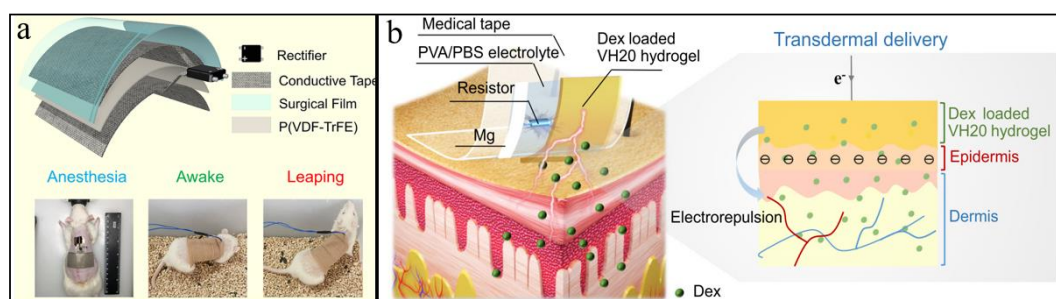


Figure 2.3 The film wound dressings(a The conductive film patch⁵⁶, b The Mg integrated patch⁵⁷)

2.3.2 Membrane

The membrane dressing is similar to a film in its ability to be semipermeable, but unlike the film, it can absorb a certain amount of water.⁶⁰ Song et al. proposed a wound dressing with a drug reservoir that took a parylene-C membrane film to separate electrolytes (deionized (DI) water) and drug solutions.⁶¹ In addition, Xu et al. integrated an electronically controlled drug release module with a battery-free, wireless wound dressing.⁶² The sensing layer consisted of a uric acid sensor, a pH sensor, and a PPy membrane coated with cefazolin antibiotics that act as the drug reservoir. The normal pH range for healthy skin and healing wounds is slightly acidic, ranging from 5.5 to 6.5. However, chronic or infected wounds that harbor significant amounts of bacteria tend to exhibit elevated pH levels above 7.3. Therefore, the signal comprising uric acid levels, pH value, and temperature will be transmitted to the central control unit (e.g., smartphone) to regulate drug release precisely. The conductive membrane exhibited great potential in tissue growth, vascularization, and collagen deposition.

2.3.3 Hydrogel

The hydrogel has a porous structure that can absorb a large amount of liquid and also allows the delivery of oxygen and water vapor. Hydrogels are generally formed by chemically or physically crosslinking polymer chains to create a three-dimensional network structure. For instance, crosslinking agents (such as N,N'-methylene-bisacrylamide, etc.) can be used to form covalent bonds between polymer chains, or physical methods such as freeze-thawing, heating, etc. can be employed to cause entanglement of polymer chains or the formation of non-covalent interactions such as hydrogen bonds. Fu et al. introduced a wound dressing that fabricated a PAM-CSS hydrogel as the base, as shown in Fig. 2.4a.⁶³ The PAM-CSS hydrogel was immersed in a solution containing Py and $\text{FeCl}_3 \cdot 6\text{H}_2\text{O}$. Finally, the color of the PAM-CSS hydrogel turned deep green, demonstrating the successful polymerization of polypyrrole (Py) in the PC hydrogel. Zhou et al.⁶⁴ reported that a wearable iontophoresis patch used Mg as an internal power source and that the viologen-based hydrogel was

used as both a drug reservoir and cathode material. The polyelectrolyte hydrogel P(AM-co-SV) composite of acrylamide (AM, offering cross-linked elastic networks) and p-styrene-bipyridine (SV, offering high redox activity) monomers. This polyelectrolyte hydrogel outperforms conducting polymers by employing a minimal driving potential for the release of drugs, demonstrating effectiveness against bacterial growth to prevent infections, and offering an optimal bioelectrical interface for efficient transdermal delivery when incorporated into the epidermal patch. After loading P (AS-co-SV) with Dexamethasone sodium phosphate (Dex), the conductivity improved to 12.4mS cm^{-1} . Wu et al. developed a thermosensitive wound dressing that used poloxamer 407-based hydrogel as the base.⁶⁵ The poloxamer 407-based hydrogel exhibits reversible thermoregulation properties⁶⁶ that can switch between fluid and semisolid states near the sol-gel transition temperature. Zhang et al. developed a hydrogel with conductivity by incorporating Zn^{2+} and PPy as conductive elements, while chitosan acts as the primary polymer backbone.⁶⁷ This hydrogel demonstrates the ability to detect changes in temperature and strain, and it promotes faster healing of infected chronic wounds when combined with ES.

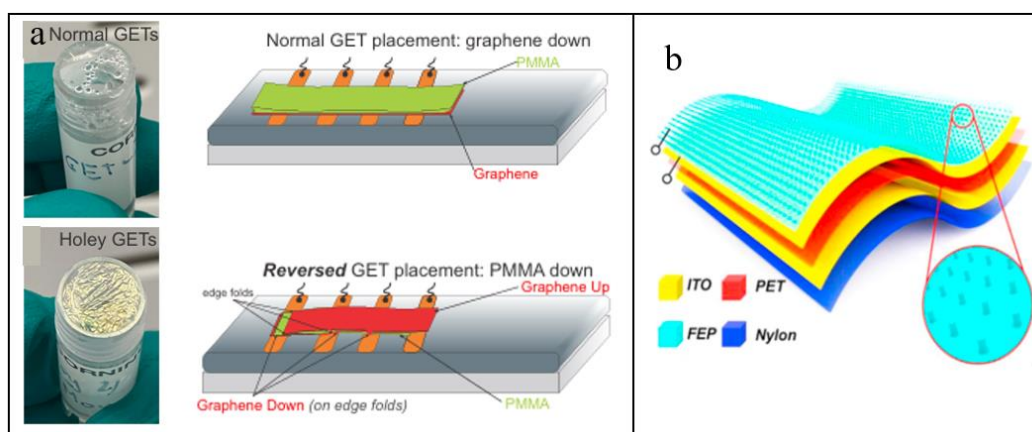


Figure 2.4 The hydrogel wound dressings(a The fabrication process of PAM-CSS hydrogel⁶³, b The hydrogel based self-powered patch⁶⁴)

2.3.4 Liquid conductive materials

With advancements in material science, liquid conductive materials (LCM) , including liquid metals, liquid organic matters and so on, endowed with remarkable

deformation and conductive capabilities, have been widely utilized in the production of flexible and wearable devices. LCM can be filled inside the elastomer and used as a stretchable circuit, or it can be printed on a smooth surface after treatment. Yang et al. present a recent development example of a highly sensitive EGaIn based capacitive strain sensor, as shown in Fig.2.5a.⁶⁸ Another widely used application for soft sensors made of liquid metals is resistance strain sensors. In addition, Kireev et al. used the Graphene to fabricated a Graphene electronic tattoos (GETs) for healthcare, as shown in Fig.2.5b.⁶⁹ Bi et al. demonstrated the development of a conductive liquid metal dressing capable of delivering antibiotics. The modification of the liquid metal with antibiotics (LA) not only enhanced its bactericidal activity, but also endowed the dressing with the ability to modulate inflammation. Zhuang et al. drew inspiration from the structure of eagle claws to develop an innovative wound dressing incorporating LCM, which creates a stable electrical field around the wound to promote accelerated healing, as shown in Fig.2.5b.⁷⁰ In comparison to traditional LCM wound dressings, the claw-inspired design utilizes hydrogel and gauze as a base, resulting in enhanced LCM stability during daily use.

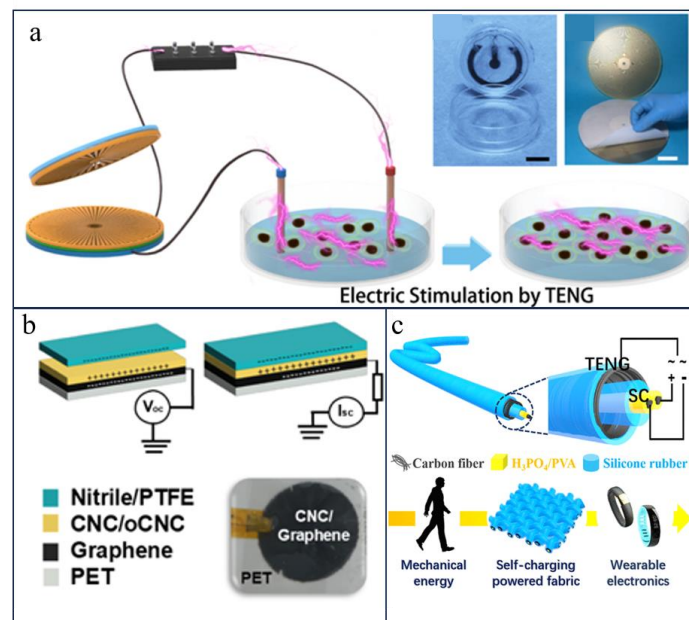


Figure 2.5 Wearable patches coated with conductive materials(a. Patch coated with graphene⁶⁸, b Self-powered patch coated with graphene⁶⁹, c Wearable devices coated with carbon fiber⁷⁰)

2.4 Wound dressings with ES

It has been demonstrated that ES plays a role in expediting the process of wound healing. However, the conventional ES treatment method requires the use of heavy devices. Thus, in recent research, many researchers have started integrating the ES function into wound dressings. Wound dressings with ES could be divided according to the power-generating method. For example, nanogenerators, such as triboelectric nanogenerators (TENGs) and piezoelectric nanogenerators (PENGs), exhibit the capability to convert physical motion into electrical power.⁷¹ Moreover, the enzymatic biofuel cell (EBFC) harnesses human biofluids, such as glucose, lactate, and ethanol in sweat, as viable energy sources. In addition to these methods, the primary method applied commercially is still external batteries.

2.4.1 TENGs

TENGs convert mechanical energy into electrical energy by harnessing the synergistic effects of triboelectrification and electrostatic induction.⁷² TENGs have a simple structure, which allows for remarkable miniaturization and fabrication using soft materials⁶¹. Additionally, TENGs generate a strong output ranging up to a few milliwatts(mW). Therefore, TENGs can be implanted to harvest energy from body/organ motion and engineered as an ideal power source for implantable biomedical devices. For instance, Zheng et al. have successfully demonstrated the use of an implanted TENG to power a pacemaker in vivo, validating the feasibility of developing TENG-based implantable biomedical devices. The sustained biokinetic energy provided by TENG would enable self-powered implantable devices.

TENGs can transform almost any mechanical motion into electrical signals^{73, 74}. Therefore, TENGs have great potential in wound healing applications, including enhancing neural differentiation of mesenchymal stem cells, converting fibroblasts into functional neuronal cells, and repairing tissue through the coupling of triboelectricity and electrostatic induction. Substantial advancements have been achieved in this field

through extensive research.⁷⁵ The working mechanism can be attributed to the coupling effects of triboelectrification.^{76, 77} When the rotation begins, an equivalent quantity of positive and negative charges is generated from copper electrodes and PTFE surfaces. At a rotational speed of 60 rpm, the short-circuit current (I_{sc}) is approximately 70 μ A. As the rotational speed increases to 140 rpm, I_{sc} reaches 100 μ A, V_{pp} reaches \sim 160V, while V_{oc} remains almost constant at any rotational speed. Yin et al. designed a wearable electrical bandage with a nanogenerator to accelerate wound healing by generating electricity from body motion.⁷⁸ This device was fabricated by overlapping the electropositive material layer made of Cu with the electronegative material layer made of Cu/PTFE and placing them on different sides of a polyethene terephthalate (PET) substrate (Fig.2.6a).

Various chemical methods can generate H_2O_2 , for example, anthraquinone-catalyzed reactions,⁷⁹ electrocatalytic reduction of oxygen, or physical methods like plasma treatment,⁸⁰ photocatalysis,⁷⁹ and piezo catalysis.⁸¹ Yuan et al. first designed a wound self-powered healing patch with ROS-responsive functionality.⁸² The ROS-responsive patch consisted of a HAP film through LBL coating 2-hydroxypropyltrimethyl ammonium chloride chitosan (HTCC), alginate (ALG), and poly-dopamine/ Fe^{3+} nanoparticles (PFNs). The ROS-responsive patch placed under the TENG, the LBL sequence as shown in Fig. 2.6c.

However, temperature is a widely prevalent factor in our everyday existence, and fluctuations in temperature can be observed in almost every aspect of surroundings. Thus, Barman et al. chose bismuth telluride (Bi_2Te_3)¹⁷, a thermoelectric material with a high Seebeck coefficient and excellent physical properties, to design a self-powered wound healing patch to generate H_2O_2 at near-room temperature.^{83, 84} According to the experiment result, Bi_2Te_3 can generate a maximum of 10 μ M H_2O_2 under varying temperature gradients. Therefore, this wound dressing patch has the ability to produce a controlled amount of H_2O_2 .

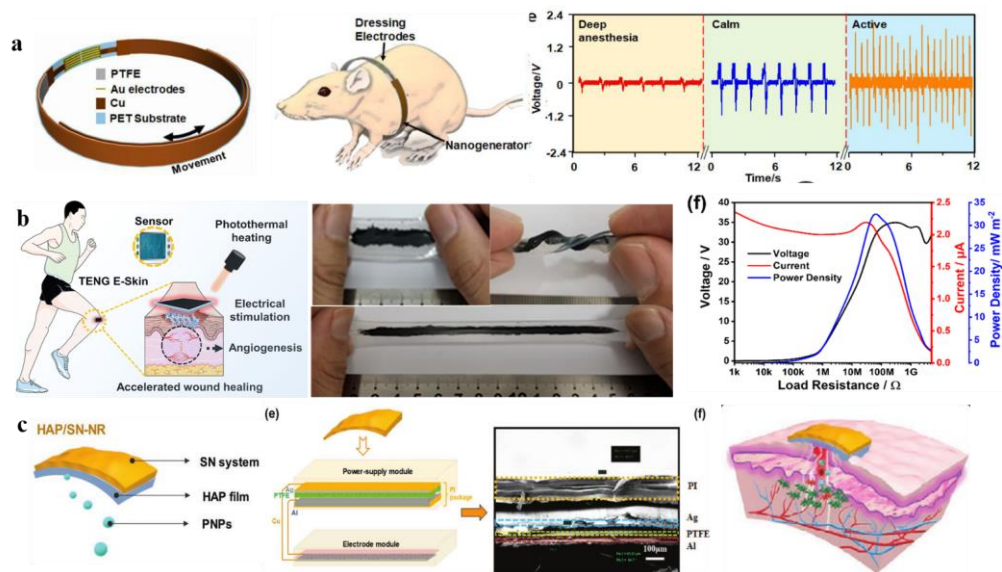


Figure 2.6 The TENGs(a Wearable electrical bandage with a nanogenerator.⁷⁸, b PPY-F127 hydrogel self-powered skin patch.⁸⁵, c ROS responsive LBL wound healing patch.⁸²)

2.4.2 PENGs

PENGs utilize the piezoelectric effect to efficiently convert mechanical energy into electricity, thereby generating sustainable and renewable power.⁸⁶ In previous studies, metal materials were employed in the fabrication of PENGs. For instance, Liu et al. developed a thin film of CuI/ZnO to harvest energy, as shown in Fig.2.6a. However, as mentioned before, metal patches are incapable of completely adapting to the flexibility and resilience of the skin.⁸⁷ To avoid this problem, Bhang et al. developed a PENG patch by aligning bidirectionally grown zinc oxide nanorods (BDG ZnO NRs) on PDMS, as shown in Fig.2.7b.⁸⁸ Each patch has a thickness of about 4.1 μm. The nine layers of the PENG patch surface generate an average voltage and current density of 1.8V and 85 nA cm⁻², respectively. The gas and liquid exchange of the PDMS layer exhibits relatively limited efficacy, potentially impeding wound respiration and hindering the process of wound healing when worn over an extended duration. Yuan et al. first designed a wound self-powered healing patch with ROS-responsive functionality.⁸² The ROS-responsive patch consisted of a HAP film through LBL coating 2-hydroxypropyltrimethyl ammonium chloride chitosan (HTCC), alginate (ALG), and poly-dopamine/Fe³⁺ nanoparticles (PFNs). The ROS-responsive patch

placed under the TENG, the LBL sequence as shown in Fig.2.7a. It is noteworthy that the PFNs within the film possess the ability to eliminate excess ROS, whereas the HAP film can selectively discharge poly-dopamine nanoparticles (PNPs) at designated injury sites for enhancing cellular well-being during transitions from neutral to slightly acidic conditions in wounds. Some nanoparticles(NPs) can enhance the piezoelectric properties of PVDF by facilitating the polarization process.⁸⁹ The reason is their capability to facilitate interactions between atoms or groups with varying charges within the molecular chain of PVDF.^{90, 91} As shown in Fig.2.7c, the nanofibers were aligned well and exhibited excellent biocompatibility.⁹¹ These nanoparticles can also serve as a modifying agent for enhancing the hydrophilicity of PVDF, thereby enabling hydrogel preparation.⁹²

Additionally, sodium alginate (SA) was utilized to create the PVDF/SA hydrogel, as shown in Fig 2.7d.³¹ In this study, the research team first employed 3D printing technology to fabricate a piezoelectric scaffold with a dual piezoelectric release model in both vertical and horizontal directions, ensuring accuracy in their findings for generating sustainable piezoelectric current. The accumulation of bacteria remains a concern for portable energy nanogenerators (PENGs). The schematic illustration and working mechanism as shown in Fig.2.7d. Hu et al. combined silver nanoparticles (AgNPs) with PVDF to create piezoelectric PVDF/Ag nanofibers.²⁵ These nanofibers were used to form a water-repellent layer. In contrast, hydrophilic polycaprolactone/Gel (PCL/Gel) nanofibers were selected as the opposite layer, as shown in Fig. 2.7e.²⁵ By assembling these two layers using the LBL technique, a Janus fibre PENG was developed. This TENG can transport wound exudate in one direction only, and the AgNPs can effectively eradicate infectious pathogens at wound sites while promoting fibroblast proliferation and migration.

Cellulose is also an ideal choice for electrospinning wound dressings due to its biocompatibility, biodegradability, excellent mechanical properties, and remarkable adsorption capability.⁹³⁻⁹⁵ Thermal therapy, including hyperthermia, has been regarded as an effective method for accelerating wound healing.⁹⁶ This is because hyperthermia has the potential to enhance blood circulation, influence enzyme functions, and trigger

Another notable advantage of EBFC is the excellent biocompatibility since high glucose and lactic acid concentrations present in human plasma can fuel electricity generation.¹⁰³ However, the electrochemical performance in the early performances was inferior. Researchers have recently significantly improved EBFC substrates, resistors, conductive materials, and enzyme protectants to overcome limitations such as short working life and low power density.^{104, 105} However, there is limited research about self-powered skin patches applied to EBFC. Therefore, researchers have gradually taken EBFC as a promising power system for self-powered skin patches.

Lee et al. first used the EBFC to stimulate cell proliferation, migration, and differentiation.¹⁰⁶ In this work, the GOX was set to generate an anodic current by glucose oxidase reaction, and the BOD was used to generate a cathodic current, followed by the reduction of oxygen. In addition, nanofiber scaffolds made of blended biopolymer (PCL-gelatin) act as the pseudo-3D matrix cues. The result indicated that electrical signals generated by the EBFC at mild levels made a significant contribution to C2C12 cellular proliferation, polarization, and migration.

In addition to using glucose directly from the blood as fuel, storing glucose in an external reservoir as a power source is also possible. In 2017, H. Kai et al. first reported an accelerated skin wound healing by a wearable patch with an integrated stretchable EBFC.¹⁰⁷ They used gellan gum and poly(acrylamide) to create a double-network hydrogel that is tough and stretchable. The hydrogel contained 17mg (94 μ ml) of fructose as the fuel reservoir, and it was immersed in a citrate buffer solution with a pH of 5 at a concentration of 200×10^{-3} mM. The dehydrogenase was taken to fabricate an anode, and BOD was used as a cathode. In this work, the electrode was fabricated with carbon fibers and coated with carbon nanotubes to immobilize the enzyme through physical adsorption in a buffer solution.¹⁰⁸ The electrodes could be used for more than 12 hours due to their large specific surface area and high conductivity. The composite of poly(3,4-dioxyethyl-eneth-iophene) and polyurethane¹⁰⁹ was employed to fabricate a 6 mm wide elastic conductive resistor with a resistance value of 10 k Ω . Applying the patch would not induce any discernible adverse effects on the integumentary system in this context. Rather than causing a rash on the skin, the hydrogel with a high

concentration (1 M) or pH (pH 7) resulted in irritation. Kim et al. also developed a pre-processed fuel reservoir, and utilize glucose as the fuel, as shown in Fig.2.8a.¹¹⁰ In this work, the Glutamate Dehydrogenase (GDH) was set as the anode and BOD as the cathode. Additionally, polyacrylamide (PAA)-PVI-[dmo-bpy2Cl]²⁺ and PAA-PVI-[dCL-bpy2Cl]²⁺, respectively, acted as mediators in the anode and cathode. These mediators were conjugated with a PEGDGE cross-linker to enhance electricity-generation longevity and electron-transfer efficiency. The biocompatible hydrogel called PAA exhibits a highly porous microstructure, the design principle. This hydrogel was immersed in a 200 mM glucose solution capable of generating a power density of 15 nW/cm². However, after 24 hours of incubation, the power density decreased to 7 nW/cm². During wound healing, hydroxides (H₂O₂) will be generated and pose a potential risk to healthy tissue while compromising the antibacterial efficacy and durability of dressings.¹¹¹ As such, removing any excess hydroxide promptly during wound treatment is imperative.¹¹² Thus, Wang et al. adopted the HRP as the cathode to regulate the accumulation of H₂O₂., as shown in Fig.2.8b¹¹³

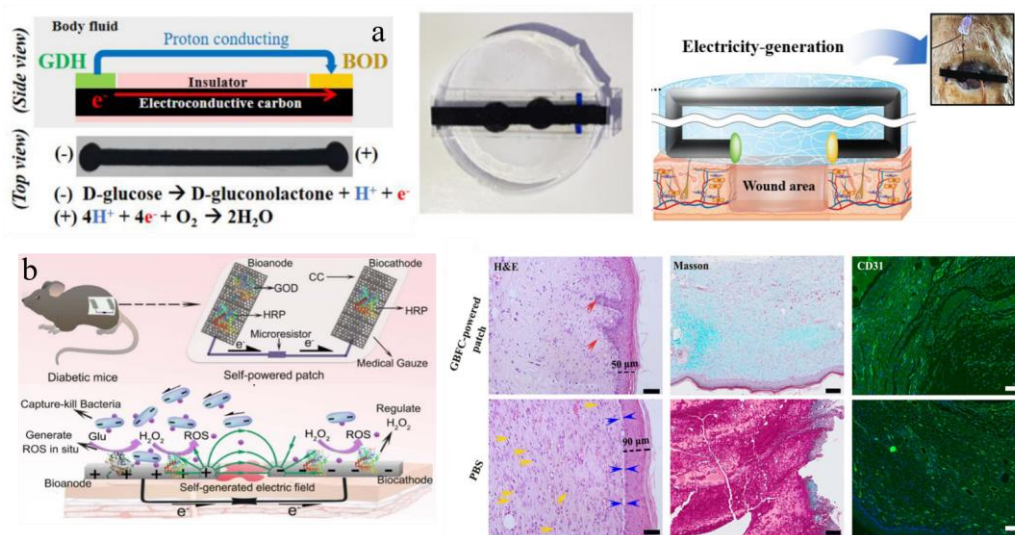


Figure 2.8 Wound dressings with EBFC (a electricity auto-generating skin patch¹¹⁰, b drug-free diabetic wound healing patch¹¹³)

2.4.4 Built-in batteries

Built-in batteries offer a notable benefit in their dependability, continuity, and

efficiency as power sources that facilitate prolonged usage with substantial dosage administration.

Procellera dressing is a commercially ES wireless device for wound healing.²² The power supply module was made of silver/zinc arrays and thin polyester cloth, which cannot generate ES for long time due to the consumption of silver/zinc arrays and the poor moisturizing ability of polyester cloth. Yu et al. used a medical cotton cushion as the substrate, the medical cotton cushion could absorb much water and keep wet for an extended time.²³ In this work, a biocompatible agglomerate was chosen to create a slurry containing AgNPs and ZnNPs, which was subsequently applied onto one side of the medical cotton cushion using a dot matrix-arrayed technique at a thickness of 2 mm. This Ag/Zn patch is moistened with sterile saline solution or water and then applied to the wound. However, this ES generation method is not convenient for wound healing. The softness and elasticity of human skin pose a challenge for metal patches to adapt thoroughly. This phenomenon is due to the significant difference in Young's modulus between metal materials and the skin. Thus, many commercial wound dressings still take the battery as the power sources due to the reliable, uninterrupted, and effective energy supplies abilities of primary batteries.⁶⁴

2.5 Conclusion

The smart wound dressings could be divided into three parts, and the conclusion of each part was shown in Table 1.

Table 1 Conclusion of smart wound dressings

Topic	Classification	Benefit	Drawback
Liquid management	Textiles	High-permeability	Low liquid absorb ability
	Microfluid channels	Directional flow of liquid	Single-functionality
Conductive wound dressing	Film	Thin	Without liquid absorb ability
	Membrane	Liquid reserve ability	Limited liquid absorption capacity
	Hydrogel	Construct a moist environment	Hard to remove after a longtime wear
	Liquid metals	Superb conductivity	Insufficient stability
Wound dressing with ES	TENGs	Electrification by friction	Unstable electrical energy generation
	PENGs	High power density	Unstable electrical energy generation
	EBFC	Relative stable power generation	Costly and low power density
	Built-in battery	Stable and high-power density	Not convenient for daily use

Wound exudates can be absorbed into microfluidic channels by surface tension. These channels, with their unidirectional structure, prevent contamination and provide a controlled environment for studying exudates, offering a promising approach to wound healing management.

(ii) Conductive performance

Conductive wound dressings can accelerate wound healing, but fabricating them has limitations. Films allow air circulation but may not remove exudates effectively, which can lead to maceration or delayed healing. Hydrogels create a moist environment but can be hard to remove due to tissue growth. PDMS, a hydrophobic material, is ideal for wound dressings as it can incorporate microfluidic channels for liquid transmission and conductive materials for conductivity. Liquid metals are effective in wound healing but lack stability; PDMS or hydrogels can be used to stabilize them. Wound dressing materials should be non-toxic, non-irritating, and have good conformability.

(iii) Combination of ES

Although there are many methods for fabricating wound dressing substrates and

self-powered systems, there are many limitations that keep them in the experimental stage, and most commercial patches for the self-powered system still use bulky batteries and the nanogenerator has many limitations.⁶⁴ The nanogenerator can't produce a stable energy output, TENGs and PENGs can't generate power when the user is static, EBFC and built-in batteries have stable power supply but their power generation materials deplete quickly, and the enzymes in EBFC are fragile and expensive, limiting its large-scale application.

The most stable option now is to use the original battery as the power source in commercial dressings, but the flexibility of the power module should be considered for better stability and comfort when worn.

(iv) Drug reservoir

In this work, the substrate was made of PDMS with good properties and easy to wear, it has unidirectional channels, PBWDP is waterproof on one side and has silver paste on the other side for various functions, this smart wound dressing is a platform and shows potential in wound healing, extending the application and providing a new therapy.

3. Methods and materials

In this work, A multifunctional wound dressing, PBWDP, was presented, featuring excellent liquid management capability, conductive and mechanical properties, as well as the ability to detect glucose level.

The substrate was fabricated using PDMS due to its excellent hydrophobicity, biocompatibility, and flexibility, making it easy to remove and wear. For the exudates absorbent ability of hydrogels, unidirectional channels were added inside the PDMS substrate that allows the delivery of blood and medicine. The PDMS was purchased in Dow Corning company, the whole name was Dow Corning DC184, and its original state was solution. In addition, the away skin side of PBWDP is waterproof and is set as a barrier to prevent outer infection. At the side of the patch near the skin, we created a serpentine path and filled it with silver paste, which can help balance the electrical field around the wound, and Ag^+ could kill bacteria. Additionally, it can be connected to external power sources to generate ES. This smart wound dressing serves as a platform that enables users or doctors to directly operate the wound (e.g., clean the wound, change medicine or ES) on the dressing during any different tissue remodeling period. In this study, the PBWDP showed great potential in wound healing, extends the application range of wound management, and provides a new therapeutic solution to promote nerve recovery and anti-bacteria.

3.1 Liquid delivery

The liquid delivery component encompasses the simulation of the micro channels, the unidirectional flow, and drug delivery. The simulation was devised to acquire an appropriate size of the micro-channels, enabling the channels to absorb the liquid instantaneously. For the unidirectional part, it could demonstrate the PBWDP with the ability of waterproof and breathability. Due to the drug delivery function of PBWDP, PBWDP is designed to be waterproof, but its waterproof function conflicts with the

drug delivery function. To solve this problem, a drug delivery system was designed, and an experiment was conducted to verify PBWDP's ability of being waterproof and delivering drugs at the same time.

3.1.1 Finite element analysis

The channel flow ability was simulated using the two-phase method of COMSOL. Nine groups with the bottom radius ranging from 0.5mm to 0.6mm were simulated by COMSOL to determine the optimal choice. Initially, the channel was filled with air. A cylinder with a radius of 1.2mm and a height of 0.2mm was designed at the bottom to simulate the blood droplet. The boundary condition at the inlet was set as pressure inlet, and the contact angle of the channel was specified as 60°. The gas is set to follow the ideal gas state equation, while for the liquid part, blood is selected. The dynamic viscosity of blood is 1.82×10^{-5} pascal-seconds and its density is 1.225 kilograms per cubic meter. Additionally, the gravity option was enabled to replicate real environmental conditions better. The whole model was meshed with a free tetrahedral mesh. Finally, submitted the program to analysis and set the analysis step at $0.25e^{-4}$ and the time period at $2e^{-3}$ in order to accurately capture microfluid behavior within the system.

3.1.2 Unidirectional liquid delivery

The static contact angle serves to characterize the wetting behavior between liquid and solid interfaces. Hydrophilic or hydrophobic properties of surfaces can be quantitatively evaluated through this parameter: surfaces with contact angles below 90° are classified as hydrophilic, while those exceeding 90° exhibit hydrophobicity. For PBWDP characterization, static water contact angles were measured at room temperature using a contact angle tester equipped with a 10 μ L droplet deposition system.

The optical system of a contact angle measurement instrument is utilized to observe and capture the morphology of liquid droplets on a solid surface. It typically

includes components such as a light source, lens, and camera to acquire clear droplet images. The droplet generation system precisely produces droplets of a defined volume and deposits them onto the solid surface. Subsequently, the captured droplet images are analyzed and processed to calculate the contact angle value.

The results of these measurements provided valuable insights into the surface properties and wettability of the material. Furthermore, real-time photo recordings were taken on the films to assess the unidirectional liquid transport capacity of specially designed channels. This allowed for a detailed analysis of how effectively and efficiently the channels facilitated the movement of liquids in a controlled manner. These experimental procedures and analyses contributed to a comprehensive understanding of the liquid delivery performance of PBWDP.



Figure 3.1 Contact angle test machine

3.1.3 Drug delivery

There are many researchers developed a drug reservoir by applying hydrogels¹⁹, metal electrodes¹¹⁴, polymers¹¹⁵, etc.¹¹⁶. However, the drug reservoir can generally only store one specific drug, for example, the anti-inflammatory or nerve repair medication. In the event of different wound healing periods, unexpected situations, and depletion of the drug supply, it may be necessary to switch medications. Those drug reservoirs, which are located near the wound, may cause secondary damage to the wound if they are frequently changed.

The wound exudates not only consist of blood, but also contains tissue fluid and other liquid. And the blood was different to the paste, that was hard to obtain. Thus, the

wound exudates that flows out after the skin was broken may contain a relatively large amount of blood, tissue fluid and other liquid, making its nature close to that of water. Thus, in this study, water was chosen to simulate blood and ink was used to enhance the visual effect to simplify the experimental process and facilitate the monitoring and analysis of the phenomena.⁷

To assess the flow capacity of PBWBP, a mixture of DI-water and red ink was used to simulate blood, while a mixture of DI-water and blue ink was used for the medicine solution. The simulated blood was dropped near the wound, and the medicine solution was released from a dropper. For drug delivery, another layer fabricated with silicone gel and channels is needed, which will be placed on the away skin side of PBWDP. In addition, a contact angle test machine was taken to detect the unidirectional delivery ability of channels inside PBWDP.

In addition, the drug delivery patch was fabricated with silica gel due to the superb softness of cylinder channels. In addition, the size of the drug delivery patch was similar to the PBWDP (length: 50mm, width: 35mm), and the location of channels corresponded to the channels of PBWDP.

3.2 Mechanical and conductive performance

One of the crucial characteristics of PBWDP was its remarkable stability when worn, which was guaranteed by a well-structured design enabling steadiness in daily life. Thus, the mechanical and conductive properties were tested by twisting and stretching.

3.2.1 Finite element analysis of mechanical performance

It is wasteful to design and fabricate any structure for testing each time. The production process requires not only materials but also time. Fortunately, the FEA software can help analyze the mechanical performance of computers. In this study, we used two finite element analysis methods in COMSOL to simulate the mechanical and microfluidic performance of PBWDP. Specifically, the mechanical performance was

simulated using structural mechanical analysis, with material PDMS and silver, respectively. One side was given a fixed constraint, and pressure at 10 KPa was applied to the opposite side to simulate stretching. The same fixed step was applied to the twisting simulation, but the difference was that the opposite pressure was applied to the two adjacent sides. The whole model was meshed with a free tetrahedral mesh. Each analysis step was set at $0.25e^{-4}$ and the time period at $2e^{-3}$ in order to accurately capture dynamic behavior within the system.

3.2.2 Conductive performance

During movement, the PBWDP deforms due to twisting or blending of the skin, causing a change in the resistance rate of silver conductive traces. A rectangular-shaped PBWDP (length: 50mm, width: 35mm) was fabricated for a tensile test with a benchtop tensile tester to evaluate its mechanical properties in terms of twisting, stretching, and blending. Two wires were connected with the silver trace, respectively serving as the anode and cathode, and encapsulated by a PMDS layer to eliminate outer disturbance. The amperemeter is associated with two wires to record the resistance change of PBWDP, as shown in Fig.3.2.

The bench-type tensile tester is usually powered by a motor, which drives the fixture to move and apply tensile force to the specimen. The tensile speed is 0.1mm/s, and the specimen is stretched by 6%, 13% and 16% of the total length of PBWDP respectively. The resistance change rate testing machine is used to measure the changes in resistance of PBWDP under different tensile conditions. By applying a constant current to the sample and using Ohm's Law ($U=IR$), the voltage drop across the sample terminals is measured to calculate the resistance.

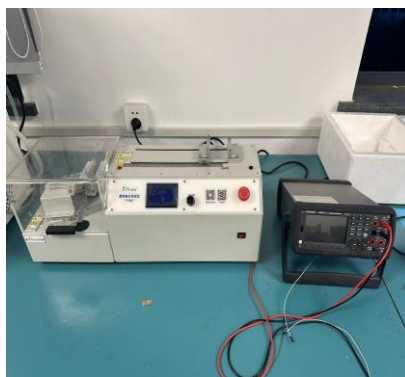


Figure 3.2 Mechanical and resistance change rate test machine

3.3 Flexible and wearable battery module

Since the self-powered skin patch with many laminations in clinical application. The performance of PBWPB under ES was assessed through the fabrication of a flexible and wearable battery module encapsulated with PDMS. The button cell SR621, sourced from Shuanglu Company for its compact size and 1.5V voltage, was utilized as the power source. The SR621 was encased in two layers of PDMS, while a carbon cloth with a thickness of 0.1mm was employed to construct a flexible electrode.

LED lights were used to demonstrate the feasibility of the flexible wearable battery module and its conductivity after being connected to the PBWDP. The PBWDP was connected to the flexible battery module with a wire, and the LED would be lighted if the flexible battery module worked.

3.4 Glucose detection

In this section, a blood reservoir was constructed by PDMS to collect the blood sample. The fabrication process closely resembled that of the blood delivery patch for PBWDP. The PDMS solution was poured into the 3D-printed module to obtain the blood reservoir. Additionally, the surface of the blood reservoir that comes into contact with the PBWDP needs to undergo hydrophilic treatment using UV light.

The glucose detection electrode was constructed using the Ni_3S_2 -coated glassy carbon electrode from our previous work. The glucose level was detected by the electrochemical workstation (CHI760E, purchased from Shanghai Chenhua Instrument

Co., LTD), as shown in Fig. 3.3.

The electrochemical workstation primarily investigates electrode processes and electrochemical reactions by applying diverse potential or current signals to the electrode system and subsequently measuring the corresponding current or potential responses. It adheres to Ohm's Law ($I = U/R$, where I represents current, U denotes potential difference, and R indicates resistance) and Faraday's Law (in the course of electrolysis, there exists a quantitative relationship between the electric charge passing through the electrode and the amount of substance undergoing electrode reaction).

When detecting the glucose level, the first step was to activate the electrode. The Ni_3S_2 -coated glassy carbon electrode was placed in the H_2SO_4 solution and activated using the cyclic voltammetry (CV) method, with an activation voltage of -1 v to 1v. The next step was to detect the glucose concentration at a working potential of 0.54 V and add the glucose solution to the blood reservoir five times, with each addition being 50 μL .

The CV method is that a linearly varying potential sweep signal is applied on the working electrode, which cycles within the selected potential range. At a specific potential, the electroactive substances in the solution undergo oxidation or reduction reactions on the electrode surface, generating corresponding currents. The magnitudes of the oxidation peak current (I_{pa}) and the reduction peak current (I_{pc}) are related to factors such as the concentration of the electroactive substance, the rate of the electrode reaction, and the diffusion coefficient. Under specific conditions, the peak current is proportional to the concentration of the electroactive substance.



Figure 3.3 Electrochemistry workstation

3.5 Construction of PBWDP

PDMS is an organosilicon compound widely utilized across various disciplines owing to its distinctive physical and chemical properties. PDMS demonstrates exceptional elasticity, facilitating effortless demolding and mold reusability. Its pliability also enables seamless adhesion to diverse substrate materials, including skin. Furthermore, PDMS showcases chemical inertness and non-reactivity with most substances, rendering it highly biocompatible and suitable for a broad spectrum of biological experiments encompassing the production of microfluidic chips. The PBWDP was fabricated by casting the PDMS solution into a 3D-printed mold.

Given the uniform distribution of PDMS, solutions were essential in preparing PMDS. The PDMS solution and curing agent (purchased from Macklin) were mixed in a weight ratio of 10:1. The mixture was then twisted for 20 minutes and placed in an oven at 60°C for 12 hours to cure. Tissue readily grows on hydrophilic materials. Thus, after prolonged use, these materials may become tightly adhered to newly formed tissues, making removal difficult and potentially causing additional harm to the healing process. Accordingly, we designed a plate with blanks to cover the PBWDP and maintain hydrophobicity in areas without channels. Next, the cured PDMS was removed from the mold and exposed to UV light (475nm wave) for 180 seconds to light the PDMS base covered with the plate. The areas that are covered with the plate stay the original hydrophobic. A 20-gauge needle was used to load 1 ml of silver paste (purchased in Selectech company) into a syringe, which was then injected slowly into the reserved serpentine trench. After drawing silver serpentine traces on the PDMS patch, it was dried at 60°C for two hours to ensure complete solidification of the silver traces. In the dynamic milieu of wound healing, the efficient and timely management of exudate is essential to prevent maceration and foster a conducive environment for tissue regeneration. Concurrently, maintaining the wound's integrity against bacterial invasion is imperative to mitigate the risk of infection, which could otherwise precipitate an inflammatory response detrimental to the healing process. Thus, it is very important to properly manage wound exudates and prevent external infections, in

addition to the unique channel design that prevents external water ingress. A waterproof solution was applied to the surface of the opposite side of PBWDP, forming an ultra-thin waterproof layer, about 1 μ m thick, which hinders water. The fabricated process is shown in Fig.3.4.

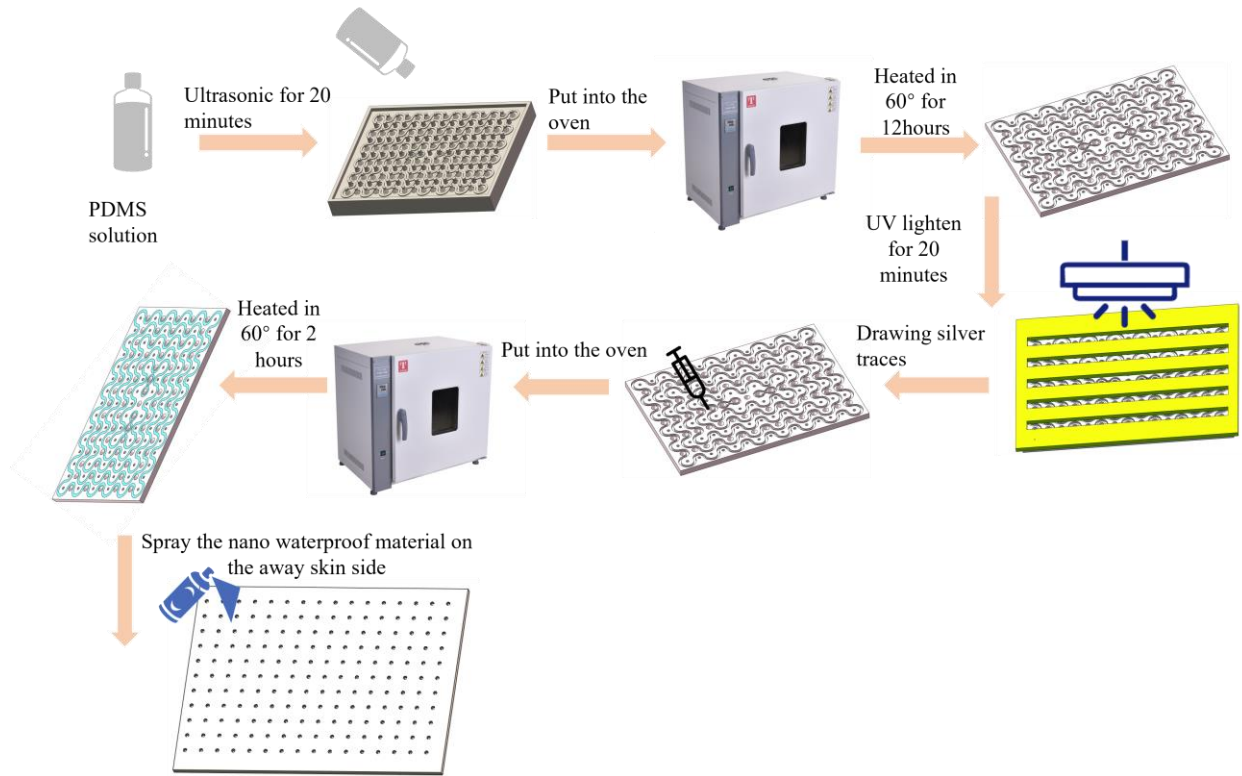


Figure 3.4 Preparation steps of PBWDP

4. Results and Discussion

4.1 Liquid delivery

4.1.1 The principle of microfluid

Some micro-channels have the ability to spontaneously absorb liquids, rather similar to a pump extracting water. The phenomenon, which is caused by surface tension making the liquid surface contract and minimize its area, is significant in micro-channels.¹¹⁷ It forms a meniscus at the liquid-air interface when in contact with the micro-channel wall and pulls the liquid into the micro-channel.⁵⁰ The absorbing capacity of a liquid is determined by its surface tension and the properties of the material. Hydrophilic materials show a strong affinity when in contact with liquids, enabling the liquids to wet the surface of the material effectively and demonstrating significant wettability. In contrast, the hydrophobic material will generate an extra force that hinders the liquid from flowing into the micro-channels. However, the inherent property of PDMS is hydrophobicity, indicating that it has limited liquid absorption capacity on its own. Nevertheless, after surface modification, the hydrophilic PDMS channels can enable self-driven liquid flow through capillary action. The principle lies in that when the liquid comes into contact with the water-wetted surface, the additional pressure (capillary pressure) generated by the surface tension can propel the liquid into the narrow channels.

In conclusion, in this work, PDMS was used to fabricate the base, and special micro-channels were designed to deliver the liquid. In addition, the surface of PDMS was modified to enhance its liquid absorption ability.

The variation in surface tension of microfluidic channels with different cross-sections results from the complex interplay between inertial migration and particle focusing. Inertial migration refers to the phenomenon where particles in a flowing fluid experience lateral forces that cause them to migrate toward specific regions within the channel, leading to their eventual focusing. This process is influenced by factors such

as flow rate, channel geometry, and particle properties. Channels with different geometries, such as rectangular, circular, or triangular cross-sections, exhibit distinct behaviors in terms of surface tension and particle manipulation. According to Fig. 4.1, particles remain mostly in the circular microfluidic channels. Therefore, in this work, circular channels were chosen to transport wound exudates and medicine.

4.1.2 Finite element analysis

PDMS is the main material for PBWDP, but it is originally hydrophobic. Therefore, in this work, we use ultraviolet light to modify its hydrophobicity to be hydrophilic, the angle change results as shown in Fig.4.2. The gap between the diameter of the inlet and outlet plays a crucial role in determining the resistance to water flow.

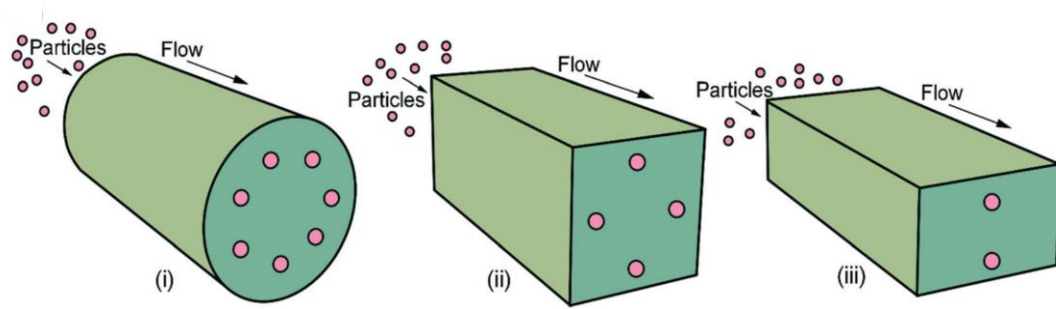


Figure 4.1 The liquid difference among microfluidic channel shapes ¹¹⁷

As shown in Fig. 4.1, the wall surface of the cylinder can adhere more particles than that of other shapes. That means the cylinder channels have good liquid transfer ability. In addition, the filling rate of the conical flow channel is 30% - 50% higher than that of the cylindrical one because the wide inlet reduces initial flow resistance, the narrow outlet provides high capillary pressure to create a self-strengthening driving force, and the high capillary pressure at the outlet counteracts gravity, making it suitable for vertical or high-flow-channel designs.

When water is absorbed from bottom to top, the height of the flow channel, h , must satisfy:

$$\frac{2\gamma \cos \theta}{r_{min}} > \rho gh \quad (4.1)$$

ρ is the density, g is the gravity, h reprints the height of the channel. r is the

minimum radius of the outlet. Theoretically, from the formula 4.1, it can be seen that the smaller the radius of the channel, the greater the liquid's absorption capacity. Nevertheless, in the actual manufacturing process, factors such as the difficulty of the manufacturing technology, the resistance to liquid flow, and the risk of blockage need to be taken into account.

The PBWDP was fabricated by introducing PDMS into the mould printed by the 3D printer, the precision of which was 0.05m. Nevertheless, the cylinder was prone to break when the width of the cylinder mould was less than 0.3mm. In addition, the especially narrow channels were prone to blockage like those channels.

The microfluid simulation results are shown in Fig. 4.3. In this simulation, the contact angle was set at 60°. We designed nine groups with different inlet and outlet radii (e.g., inlet diameter in the bottom at 0.5mm, outlet diameter in the top at 0.9mm, denoted as B0.8-T0.4). It can be seen that the design with a top radius of 0.35mm and a bottom radius of 0.45mm had a faster absorption speed than the other eight groups, and the water could not flow back. Increasing the gap between the diameter of the inlet and outlet led to an increase in resistance, resulting in some being unable to flow through the channel. In the drug delivery channel, the bottom radius was larger than that of the blood channel, enhancing drug delivery efficiency.

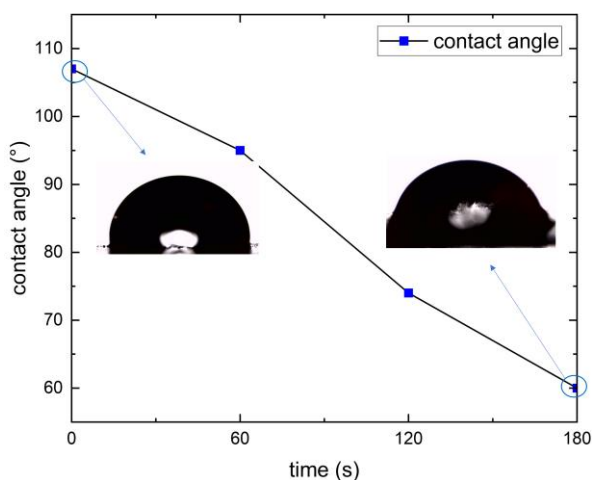


Figure 4.2 The contact angle changed rate under UV light

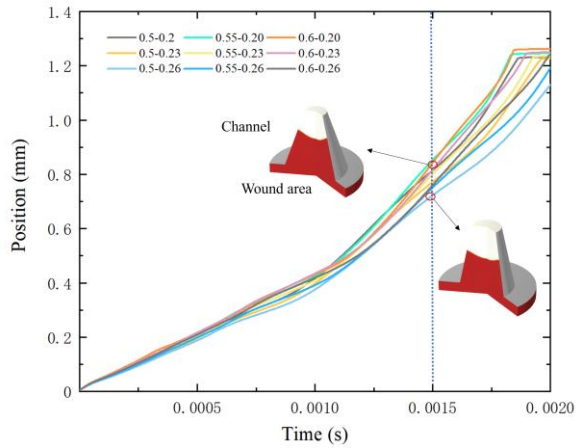


Figure 4.3 The flow rate of different channel

The PBWDP has a porous structure that provides good breathability to promote oxygen perfusion into the wound and create a moist environment. Except for B0.6-T0.2 channels, PBWDP used another shape channel, T0.6-B0.4, to enhance breathability and drug delivery ability. Waterproof medical tape, single B0.8-T0.2 channel patch, and PBWDP were divided into three groups, covered on a bottle filled with DI water, then put in an oven at 60°. In the first three hours, all three groups showed similar weight loss rates. The results as shown in Fig.4.4. After 36 hours, there was no water in the bottles covered with PBWDP, indicating that PBWDP had better air permeability than the other two groups.

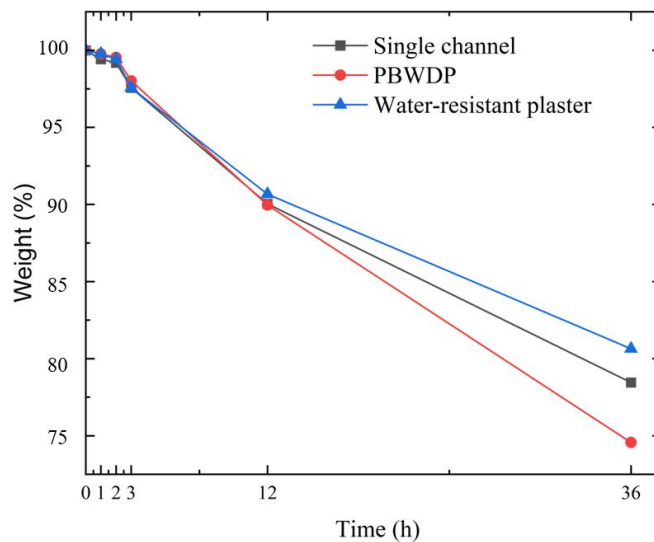


Figure 4.4 Weight loss rate

4.1.3 Unidirectional liquid delivery

Waterproof dressings are of vital importance for wound healing. Water serves as

the medium for bacteria to survive and spread.^{60, 118} Dressings can prevent external moisture from reaching the wound, keeping it relatively dry and reducing the chance of bacteria invading through water, such as avoiding contact with sewage and lowering the risk of infection. At the same time, they can prevent sweat and urine from soaking the wound, maintaining the stable microenvironment necessary for wound healing and preventing tissue cells from becoming fragile due to water immersion, indirectly preventing infection. Moreover, dressings can prevent scabs or newly formed tissues from being damaged by water infiltration, protecting the wound's own barrier function, blocking direct bacterial invasion, and reducing the chance of infection.

However, most have poor liquid transfer. With microfluidic tech progress, various micro channels exist for one-way liquid flow. Therefore, micro channels were designed to improve transfer ability in this study. In order to test the liquid delivery ability of PBWDP, an experiment focusing on water droplet permeation and reverse osmosis was carried out. The water droplet was then dropped onto the inlet of the blood channel. Fig.4.5 demonstrated that the droplet could rapidly flow through the blood channel on the side near the skin of PDWBP, but it was blocked on the opposite side of PBWDP. This illustrates that the channel could meet the requirement of unidirectional flow.

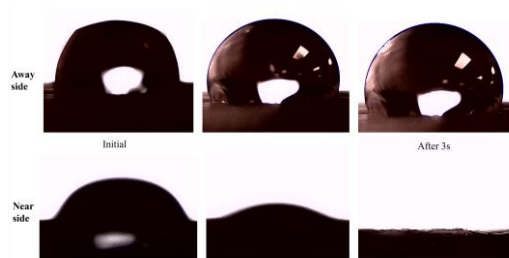


Figure 4.5 Water delivery ability of the channel

However, there are many complicated factors in the actual use process. Consequently, an additional experiment was conducted to assess the unidirectional delivery capability of PBWDP. A foam material was utilized as a skin analog due to its numerous small wrinkles and limited water absorption properties akin to human skin. Fig.4.6 and Fig.4.7 present the findings of the PBWDP experiment, both with and without the inclusion of silver traces. The results clearly demonstrate that regardless of the configuration, red-dyed water does not seep through from the side opposite to the

skin. However, it is evident that there is permeation through the side near the skin. This observation suggests that PBWDP provided a potential barrier effect in preventing liquid penetration from one direction while allowing it from another.

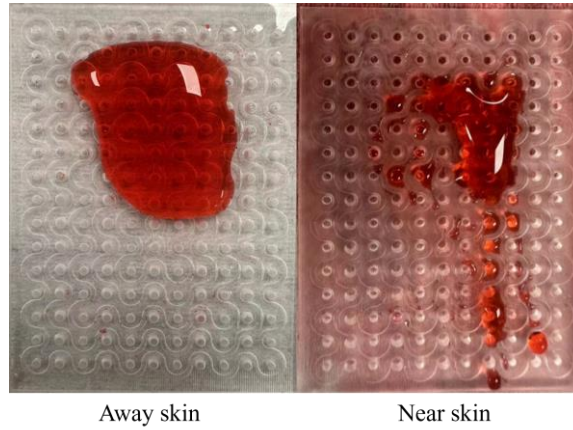


Figure 4.6 Blood simulation of the patch

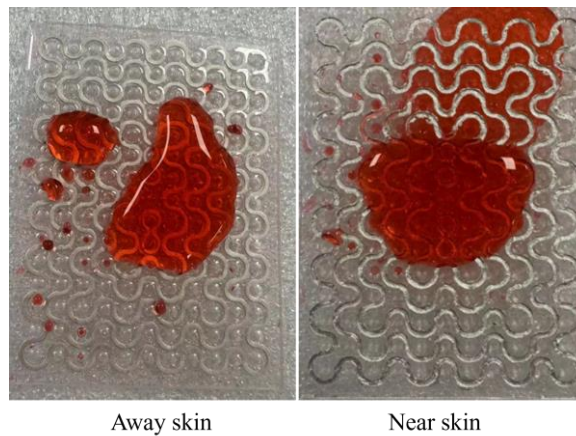


Figure 4.7 Blood simulation of the PBWPD

4.1.4 Drug delivery

The special waterproof design of PBWDP ensures that only additional passive forces can effectively deliver the drug to the wound. To enhance the ability of the drug delivery system, a drug delivery layer fabricated with a silicone gel layer and drug channels corresponding to the B0.4-T0.2 channels of PBWDP has been carefully fabricated. The unique structure of the B0.4-T0.2 channels allows for a sharper decline degree, making them more likely to absorb liquid from the top. Moreover, the reduced aperture size served to augment the inlet pressure, thereby fortifying the barrier's efficacy against external contamination. A dropper filled with blue ink and anti-

inflammatory drug solutions is placed on top of the silicone rubber layer. A force is then applied to squeeze out these solutions through the drug channels. In this process, drugs would flow through the PBWDP to reach the wound area under microfluidic force and extrusion force, as depicted in Fig 4.8. The silicone gel layer will enhance capillary force when passing through PBWDP, and it is soft, which will reduce discomfort. In addition, the medicine could not flow through the drug delivery patch without extra pressure, as shown in Fig 4.9, which also prevented other outer liquids from being infected when the medicine was delivered to the wound.

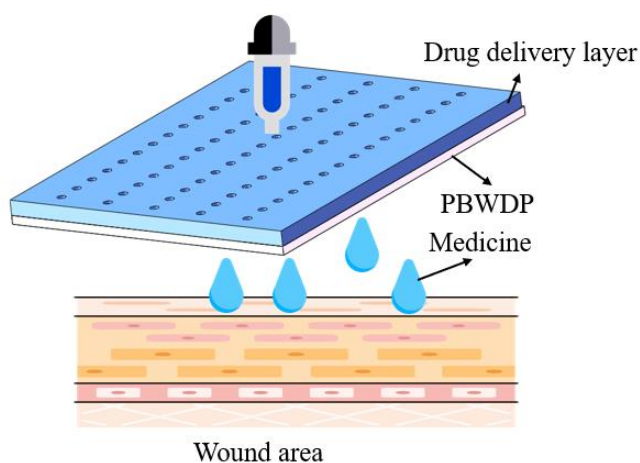


Figure 4.8 The working schematic diagram of the drug delivery layer

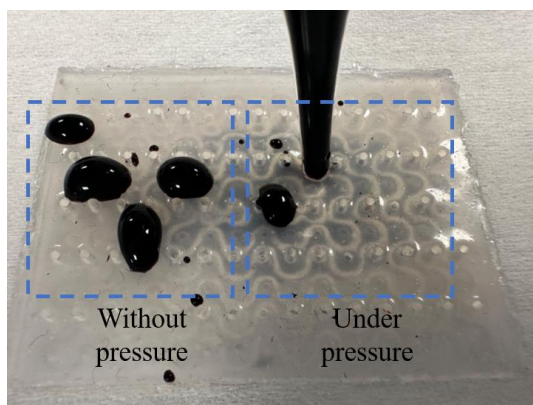


Figure 4.9 Drug delivery results

4.2 Mechanical and conductive performance

4.2.1 Finite element analysis of mechanical performance

Since silver has a superb conductive rate and is equipped with the ability of anti-bacteria, it was considered as the conductive material for fabricating the PBWDP. Silver paste was applied in the reserved grooves, and the conductive silver traces were obtained when the silver paste solidified. The snake demonstrates excellent flexibility and robustness. Thus, in this work, the snake-like silver traces were designed to fulfill the conductive functions. And the rectangle silver traces were designed to compare the stability of the snake traces. The silver traces were set between the outlets of the two channels. The gap between the two outlets was approximately 2.2mm. Taking into account the stability, manufacturing difficulty and precision, the width of the silver traces was set at 1.2mm.

In the mechanical performance, the long and short sides were fixed, and a pressure of 10 KPa was applied to the opposite sides to test their stretchability. Fig.4.10 illustrates that the patch with silver trace had a bigger displacement in both directions under the same pressure, demonstrating that its stretchability was better than the patch with rectangle traces. In addition, the extrusion ability was tested by applying a force of 10N/m^2 . Fig.4.11 and Fig 4.12 illustrate the stress distribution of rectangle and snake traces. The average stress distribution of rectangle traces was higher than that of snake traces, and high-stress regions appeared in the corners of rectangle traces, adding to the risk of break for conductive line.

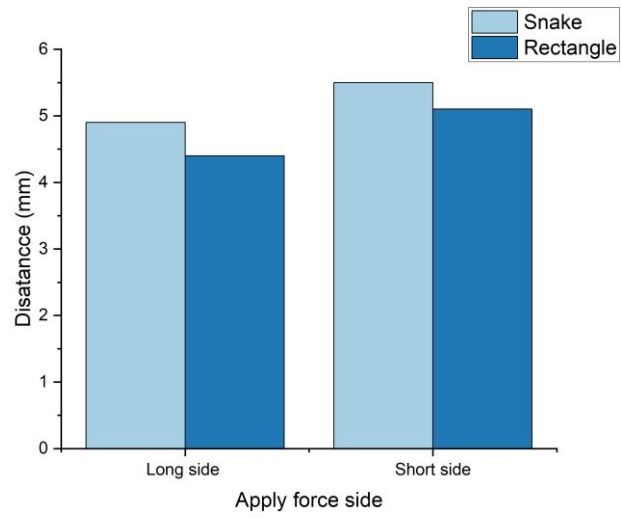


Figure 4.10 The displacement difference between two instance

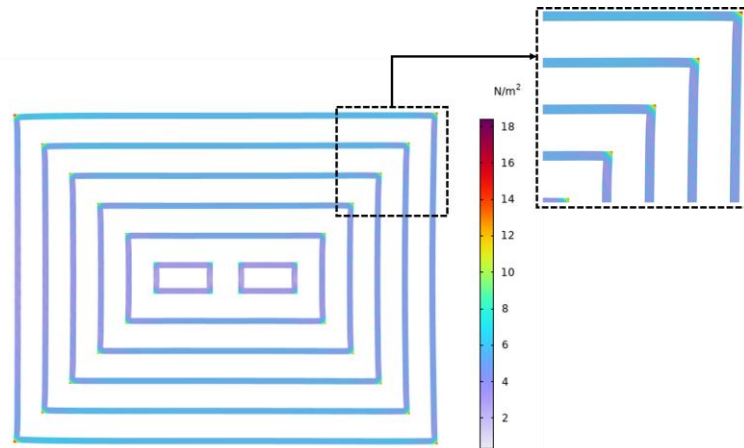


Figure 4.11 The extrusion resultl of rectangle traces

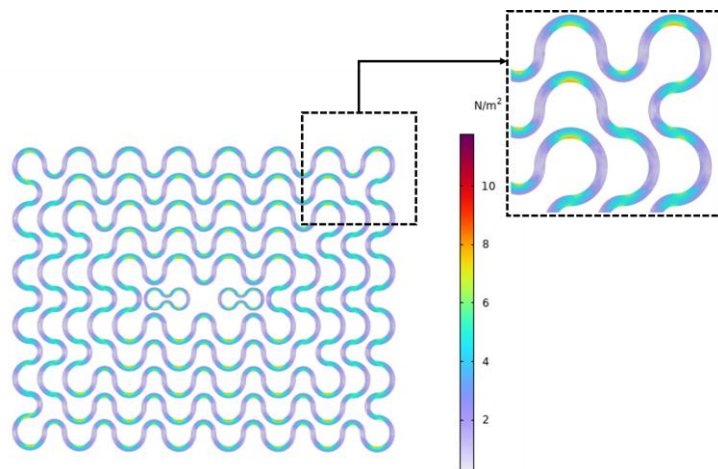
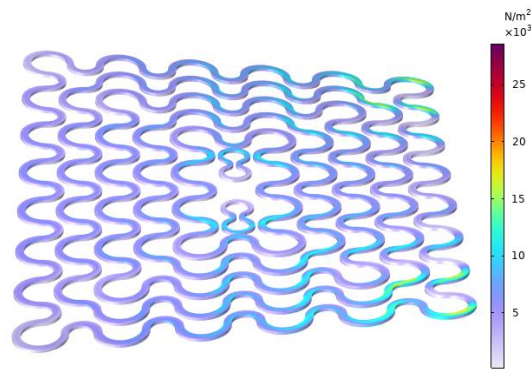
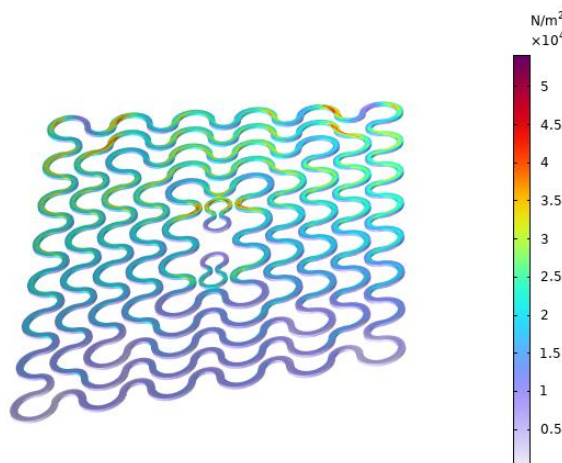


Figure 4.12 The extrusion resultl of snake traces

Although the stress value at the corner of the snake traces was higher than the stress value in the surrounding area, it was less than the average stress of the rectangle traces. Consequently, the snake traces exhibited a lower risk of breaking when compared to rectangle traces. In addition, the twisting performance was also simulated. In the twisting simulation process, a fixed load was applied to one side of PBWDP, and a 1000N/m^2 reverse direction force was applied near both sides of the fixed side. The stretching and twisting simulations were performed according to the long and short sides, respectively. The Fig.4.13 showed the stretching results.



a Stretching on the long side



b Stretching in the short side

Figure 4.13 Stretching results of snake traces

The mechanical performance of PBWDP was also simulated. For the stretching ability test, a fixed load was applied to one side of PBWDP, and a load of 500N/m^2 was

applied to the opposite side. For the twisting ability simulation, a fixed load was also applied to one side of PBWDP, and forces of 1000N/m^2 were applied in opposite directions near the two sides of the fixed side which was similar to the simulation of silver traces. The stretching and twisting simulations were performed according to the long and short sides, respectively.

According to the results calculated in COMSOL (Fig. 4.14), the stress showed uniform dispersion in all groups. In both the twisting and stretching processes, the outer silver conductive trace experiences higher stress because this region is the main area of transformation. The high-stress region mainly consists of the corner of the trace. However, this phenomenon will be improved on the long side of PBWDP. Furthermore, the stretching simulation results indicated that a high-stress region also existed in the corner area. At the same time, the stress in the inner area was much lower than that in the outer loop. The results demonstrated that the inner area, mainly focused on the wound area, had greater durability due to experiencing lower stress. In addition, the tensile strength of PDMS typically falls within the range of several MPa, which ensures that the resulting stress on the PBWDP remains within a reasonable and safe limit post-deformation.¹¹⁹ The special snake-traced design not only enables better mechanical performance of silver conductive traces when deforming the PBWDP, but it also provides enhanced flexibility and durability. This innovative design has significantly improved the wear and tensile properties of the material, making it more resistant to damage or breakage during use.

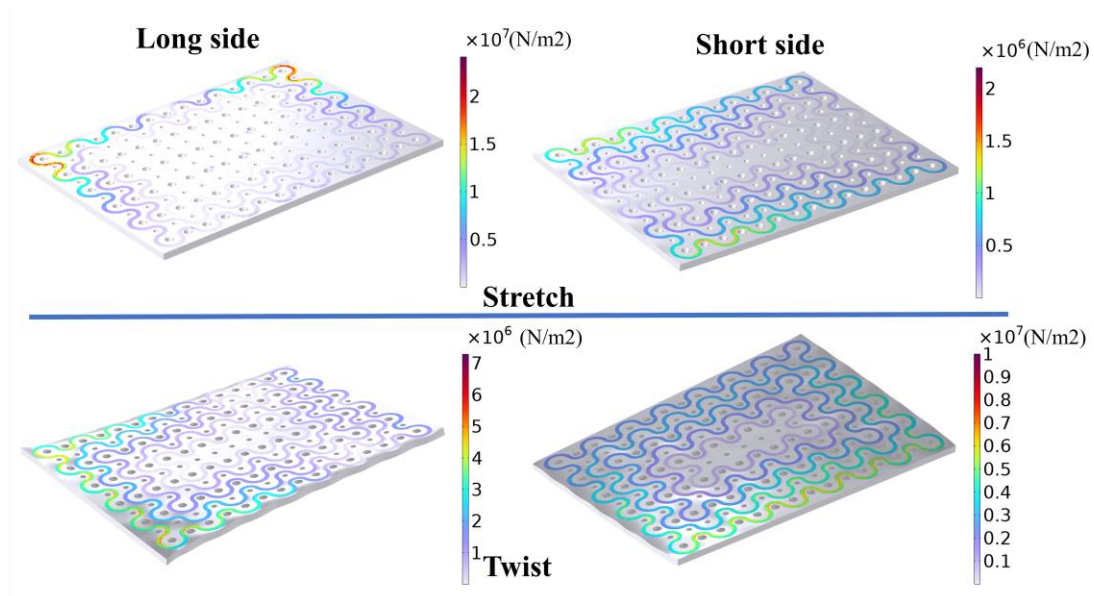


Figure 4.14 The comparison of twisting between simulation and experiment

Additionally, the increased stability and reliability of PBWDP with snake traces make it a reliable choice for various applications. Furthermore, the unique shape of the snake traces allows for more area contact with wounds compared to traditional rectangle traces. This may contribute to its stronger antibacterial property, as it can effectively inhibit bacterial growth and promote faster healing. In conclusion, the incorporation of snake-traced designs in PBWDP has proven to offer improved mechanical performance, stability, reliability, and antibacterial properties.

4.2.2 Conductive properties

Once applied to the wound site, PBWDB will be deformed by the pressure of the surrounding tissues and the traction of the human body during movement, resulting in an impact on electrical conductivity. Therefore, it is necessary to take into consideration the influence of stretch and twist on the PBWDP. A mechano-electrical measurement was conducted in order to measure the conductivity of PBWDP by taking a 50×37 mm piece coated with silver paste and connecting a conductive line in the outer silver trace area for testing its conductive property.

As shown in Fig.4.15, after a total of 60 cycles of use, the PBWDP was able to maintain its initial resistance state without huge degradation. This demonstrates the

durability and reliability of the PBWDP over an extended period of time. The ability to consistently retain its original resistance state after numerous cycles further highlights the high quality and performance of the material. Although the resistance changed significantly to 13.5Ω under the 16% stretch rate, it still remains within a reasonable range.

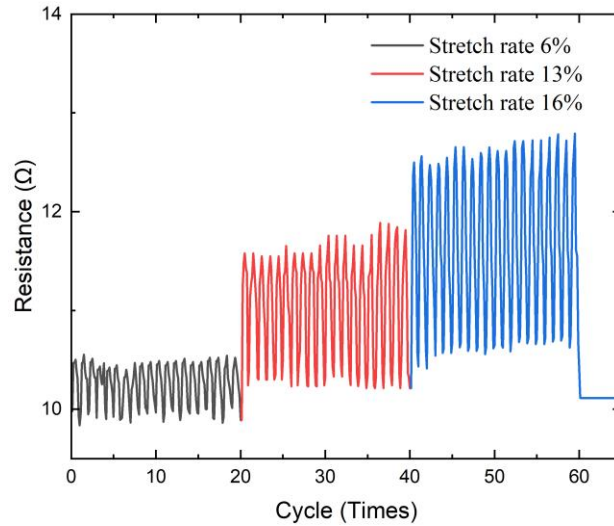


Figure 4.15 Resistance change rate under stretching

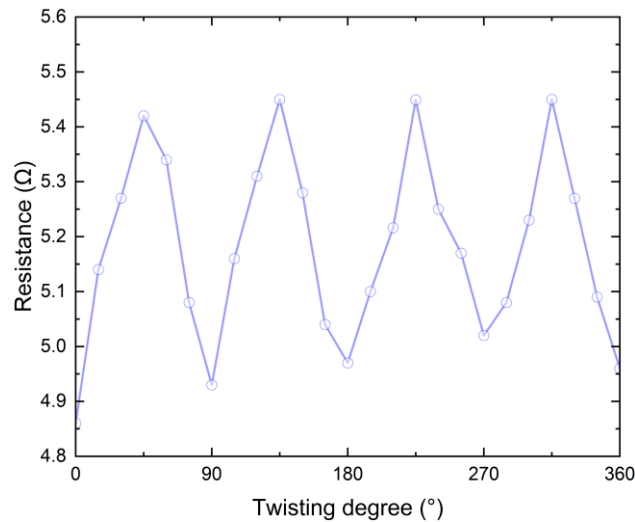


Figure 4.16 Resistance change rate under twisting

Additionally, the twisting results are shown in Fig.4.16. The PBWDP was twisted 15° each time, and the electrical resistance value was recorded. After a 90° twisting cycle, the twisting process of PBWDP will pause for a second. When twisting the PBWDP, the resistance will increase by about 9%, but when the PBWDP is in a stable status, the resistance will recover the original state. Upon torsion of the PBWDP, an

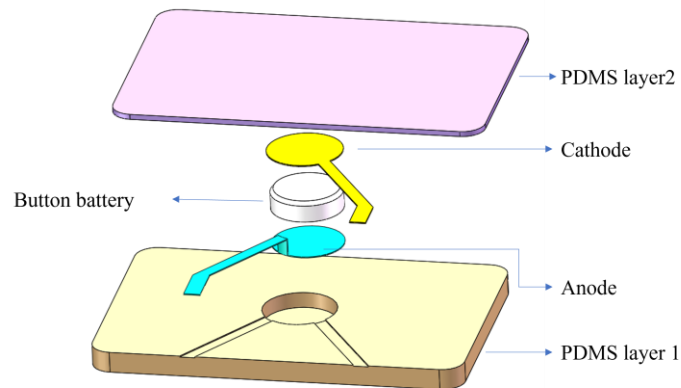
approximate 9% increment in resistance is observed. However, once the PBWDP attains a quiescent state, the resistance reverts to its initial condition. The findings demonstrated that the distinctive snake trace within the PBWDP facilitates a negligible alteration in resistance upon twisting. In conclusion, the special silver snake trace had a lower resistance change rate that enabled the stability of ES when exercising.

4.3 Flexible and wearable battery module

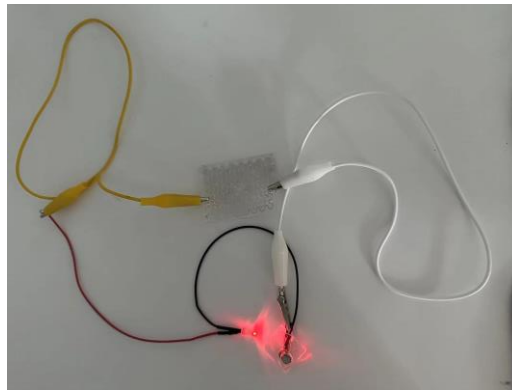
Nanogenerators have limitations, such as low power density and an unsustainable power supply.^{64, 120} The original batteries are bulky and not convenient for long-term wearing, which can be a major inconvenience for users who rely on wearable devices. To solve this problem, a solution was proposed that encapsulates the button battery with PDMS and took carbon cloth as the anode and cathode. The button cell was used to power the watch, with small size. This innovative approach not only reduces the size and weight of the battery, making it more comfortable for long-term wearing but also ensures a reliable power supply for the wearable device. By encapsulating the button cell with PDMS, we provide a protective barrier that enhances durability and longevity. Additionally, coating it with liquid metal as the conductive material as the electrode improves flexibility. In addition, to establish a connection between the battery and the patch, we incorporated a conductive stripe at the top and maintained a conductive area without PDMS, as illustrated in Fig.4.16a.

The button cell has a small size, with a radius of 3.3mm and a thickness of 2mm, and it provides a convenient, long-lasting power supply with a voltage of 1.5v. In this experiment, the LED was chosen to directly demonstrate the conducting state of PBWDP, with a working voltage range of 1.8v to 2.4v. Consequently, two button cells were utilized for the experiment. The results depicted in Fig. 4.17b demonstrate the power supply and conductive capability when PBWDP is worn on a fake silicone gel-made arm. The LED could be powered up, highlighting the efficiency and potential practicality of the power module and skin patch system. Additionally, it is noteworthy

that even when subjected to twisting or bending, the LED maintained its original level of brightness, indicating the robustness and durability of this technology.



a The schematic diagram of a flexible battery



b The light image of the LED

Figure 4.17 The flexible battery

When administering ES to a wound, it becomes necessary to modify the shape of silver traces in PBWDP. This is due to the fact that the electric current invariably seeks the shortest route, which consequently does not encompass the entirety of the wound area, as illustrated in Figure 4.18.

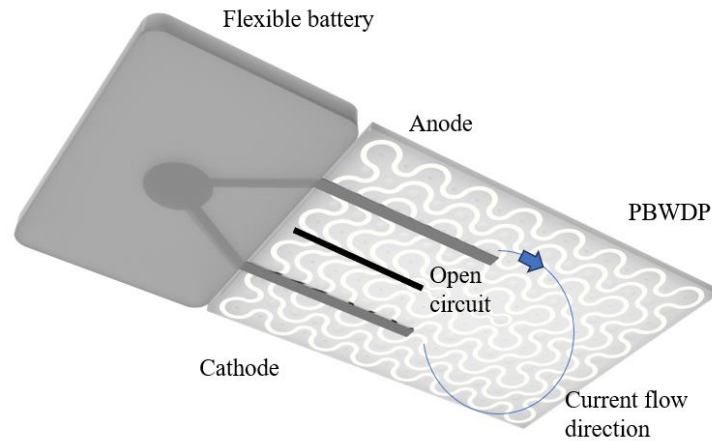
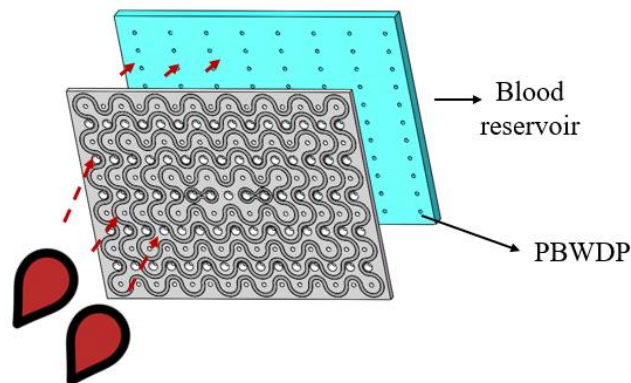


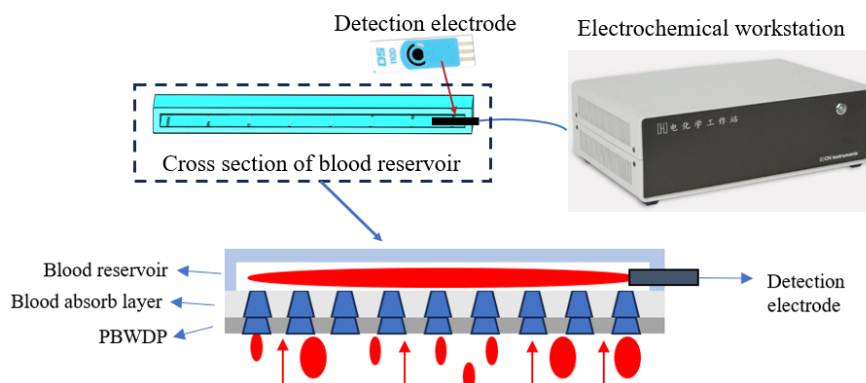
Figure 4.18 The working principle of PBWDP

4.4 Glucose detection

Blood is a classic analyte widely used in medical testing and diagnostic procedures, containing a wealth of information about the healthy condition of individual, including levels of various hormones, nutrients, and waste. However, glucose tests always require puncturing the skin to collect blood, which is painful. During the initial stage of wound recovery, a lot of blood will be generated by the wound. This blood can be collected and regarded as an ideal sample for detecting certain items. Therefore, the PBWDP was equipped with a blood bank to quickly collect blood and analyze glucose level. Fig.4.19 illustrated the working mechanism, showing the blood flow from the PBWDP to the blood reservoir and then demonstrating how the detection electrode can be inserted into the reservoir to detect the glucose level.



a The working schematic diagram of the blood reservoir



b The schematic diagram of glucose detection

Figure 4.19 The process of blood absorb and detection

During the detection process, the first step was to add 1.25mL of DI-water onto the blood absorb layer, followed by adding 250 μ L of 1mmol/L glucose solution. It was evident from Fig.4.20 that the current increases immediately and significantly each time a glucose solution was added, indicating that the sensor responded quickly. The current then showed a stable trend until the next addition, demonstrating consistent and reliable performance of the detection system.

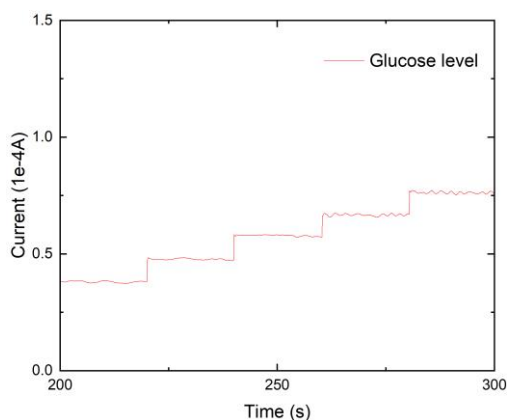


Figure 4.20 The results of glucose level detection

In addition, three PBWDPs filled with solutions of different glucose levels were tested to validate the accuracy of glucose detection. Add 1.25ml of a glucose solution containing components 0.167 mmol/L, 0.375 mmol/L, and 0.5 mmol/L to the near skin side of PBWDP. And the glucose concentration was corresponded to that of the reference group after addition of 250 μ L, 750 μ L and 1250 μ L.

Figure 4.21 showed the glucose test results at different glucose concentrations, and also provides a comparison with the results of previous experiment. The results showed

a certain degree of agreement with the historical data, that proven that the PBWDP could support a stable environment for glucose detection. Since the glucose detection relies on a redox reaction, it was imperative to maintain a stable environmental context that remains inert to the reaction dynamics. This ensures the accuracy and reliability of the glucose measurement process.

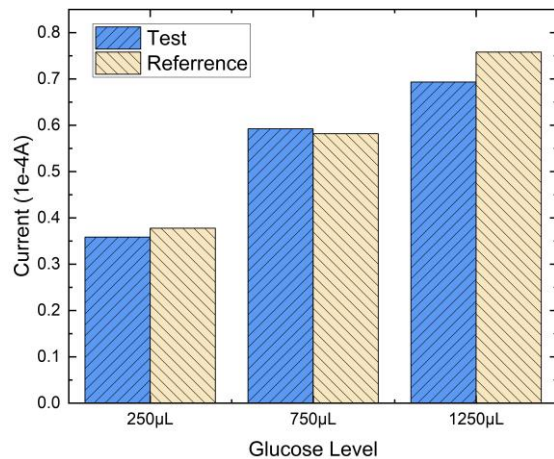


Figure 4.21 The results of glucose level detection

5. Conclusion

The skin is the largest defense against the external environment, but some ignore wound significance which can cause complications, many researchers developed wound dressings, there are problems with nanogenerators, and a PDMS-based wound dressing with special channels was designed and investigated in four aspects.

(i) Liquid management

To efficiently absorb wound exudates, we have developed specialized drug delivery channels, which not only facilitate the removal of liquid from the wound but also enable oxygen delivery. Several channel groups have been simulated using COMSOL to ascertain the most optimal configuration. In addition, both sides of PBWDP have been treated with UV light and a nano-waterproofing reagent to ensure effective liquid management. Thus, PBWDP could expel blood and prevent the entry of external fluids to a large extent. PBWDP has the capability to extract blood and significantly impede the infiltration of exogenous fluids.

(ii) Mechanical and conductive performance

In this part, we constructed a silver-trace-decorated PDMS patch to enable the conductivity of PBWDP. The first step was to test the shape of silver traces. Two silver traces were simulated by COMSOL to obtain the optimal shape with superb deformation performance. The next step was to evaluate the conductivity performance of PBWDP under deformation. The PBWDP was stretched and twisted using the tensile bench, and the resistance rate was recorded. The results showed that the PBWDP with silver snake traces exhibited better mechanical performance than the PBWDP with silver rectangle traces. Additionally, the PBWDP was able to maintain its original resistance rate after prolonged mechanical activities.

(iii) Flexible and wearable battery

Instead of fabricating a self-powered system to support the ES function, a flexible battery was constructed to maintain a stable power supply in this work. The flexible battery consisted of a button cell, carbon cloth, and two PDMS layers. The button

battery is only 6.2 mm in size, which is about the size of a mung bean. Additionally, both the carbon cloth and the PDMS are made of flexible materials that enhance the flexibility to a large degree.

(iv) Glucose detection

Since blood is the ideal analyte for testing glucose levels, we fabricated a blood reservoir to collect the blood for glucose detection. After the blood collection, glucose level detection was conveniently performed by inserting the detection electrode into the blood reservoir, resulting in the display of glucose levels.

In conclusion, the PBWDP design was inspired by toy bricks, and users can add functional modules according to their real situations, which proposes another new perspective for smart dressing in wound management. In addition, the channels of PBWDP were hydrophobic, which means the tissue will be hard to grow in the channels, reducing the secondary damage when the PBWDP is removed for a long time.

6. Discussion

In this study, there are several limitations that need to be addressed in the future work. First, the silver paste was only used to construct flexible conductive wires in order to find the best conductive method. Furthermore, the silver paste usually contains toxic additives. However, the toxic additives were disregarded and no measures were taken to reduce them. In future studies, additional procedures will be adopted to prevent toxicity. The inert coating represents a favorable approach to prevent toxicity and guarantee that the silver trace will not undergo corrosion or oxidation. For instance, an ultra-thin silica coating can be fabricated by chemical vapor deposition (CVD). The life and safety of the flexible battery module need a comprehensive and long-term experiment due to many factors, and only through such a meticulous and prolonged test can its durability and safety be precisely assessed to lay a solid foundation for wide application and commercialization. Manual operation of the drug delivery system which could be improved by a PDMS reservoir, and the integration of the glucose detection module which could be combined with a flexible PCB plate for a mobile

detection platform.

In the future, when it comes to large-scale commercial applications, metal molds can be used to replace the existing resin molds. Employing laser technology to process metal molds can endow the mould with higher precision, which could enable the PBWDP to have more channels, thereby enhancing the breathability of PBWDP. PDMS is an inert material whose performance is not readily affected by factors such as sweat. Hence, it is suitable for long-term use. And other additives could be added to the PDMS solution to enhance its durability and antibacterial ability. Nevertheless, enzymes could be supplemented to address the issue of flow channel blockage after blood coagulation. Since some enzymes consider blood as fuel and generate water. Under the capillary pressure of the unidirectional channel in this work, the water is capable of removing the blood in a timely manner to keep the channel from being blocked by the blood.

The metal mould can be employed multiple times and maintain its original performance following successive sterilization cycles. The manufacturing cost of PBWDP will be considerably reduced as only PDMS and silver paster are necessary for production. The production process is relatively simple to operate, endowing the PBWDP with great potential for future commercial applications.

Another important question is that the relevant biocompatible experiments need to be done to demonstrate that the PBWDP will not have a negative effect on users. Since, the manufacturing process of PBWDP is not totally similar to others, which may affect biocompatibility and user safety, making these specific experiments essential.

In the future work, the PBWDP could equip a self-power system that will replace the flexible battery module. And the enzyme could be integrated into the PBWDP to enable the PBWDP with the self-clean ability.

Reference

1. Yu, R.; Zhang, H.; Guo, B., Conductive Biomaterials as Bioactive Wound Dressing for Wound Healing and Skin Tissue Engineering. *Nanomicro Lett* **2021**, *14* (1), 1.
2. Colonna, M., Skin function for human CD1a-reactive T cells. *Nat Immunol* **2010**, *11* (12), 1079-80.
3. Strodtbeck, F., Physiology of wound healing. *Newborn and Infant Nursing Reviews* **2001**, *1* (1), 43-52.
4. Harper, D.; Young, A.; McNaught, C.-E., The physiology of wound healing. *Surgery (Oxford)* **2014**, *32* (9), 445-450.
5. Nethi, S. K.; Das, S.; Patra, C. R.; Mukherjee, S., Recent advances in inorganic nanomaterials for wound-healing applications. *Biomater Sci* **2019**, *7* (7), 2652-2674.
6. Schaper, N. C.; van Netten, J. J.; Apelqvist, J.; Bus, S. A.; Fitridge, R.; Game, F.; Monteiro-Soares, M.; Senneville, E.; Board, I. E., Practical guidelines on the prevention and management of diabetes-related foot disease (IWGDF 2023 update). *Diabetes Metab Res Rev* **2024**, *40* (3), e3657.
7. Li, Z.; Fan, X.; Luo, Z.; Loh, X. J.; Ma, Y.; Ye, E.; Wu, Y. L.; He, C.; Li, Z., Nanoenzyme-chitosan hydrogel complex with cascade catalytic and self-reinforced antibacterial performance for accelerated healing of diabetic wounds. *Nanoscale* **2022**, *14* (40), 14970-14983.
8. Gurtner, G. C.; Werner, S.; Barrandon, Y.; Longaker, M. T., Wound repair and regeneration. *Nature* **2008**, *453* (7193), 314-21.
9. Ou, Q.; Zhang, S.; Fu, C.; Yu, L.; Xin, P.; Gu, Z.; Cao, Z.; Wu, J.; Wang, Y., More natural more better: triple natural anti-oxidant puerarin/ferulic acid/polydopamine incorporated hydrogel for wound healing. *J Nanobiotechnology* **2021**, *19* (1), 237.
10. Augustine, R.; Gezek, M.; Seray Bostanci, N.; Nguyen, A.; Camci-Unal, G., Oxygen-Generating Scaffolds: One Step Closer to the Clinical Translation of Tissue Engineered Products. *Chem Eng J* **2023**, *455* (Pt 2).
11. Junker, J. P.; Kamel, R. A.; Caterson, E. J.; Eriksson, E., Clinical Impact Upon Wound Healing and Inflammation in Moist, Wet, and Dry Environments. *Adv Wound Care (New Rochelle)* **2013**, *2* (7), 348-356.
12. Qazi, T. H.; Rai, R.; Boccaccini, A. R., Tissue engineering of electrically responsive tissues using polyaniline based polymers: A review. *Biomaterials* **2014**, *35* (33), 9068-9086.
13. Park, S. S.; Kim, H.; Makin, I. R.; Skiba, J. B.; Izadjoo, M. J., Measurement of microelectric potentials in a bioelectrically-active wound care device in the presence of bacteria. *J Wound Care* **2015**, *24* (1), 23-33.
14. Ojingwa, J. C.; Isseroff, R. R., Electrical stimulation of wound healing. *J Invest Dermatol* **2003**, *121* (1), 1-12.
15. Thakral, G.; Lafontaine, J.; Najafi, B.; Talal, T. K.; Kim, P.; Lavery, L. A., Electrical stimulation to accelerate wound healing. *Diabet Foot Ankle* **2013**, *4*.
16. Zhang, X.; Wang, Z.; Jiang, H.; Zeng, H.; An, N.; Liu, B.; Sun, L.; Fan, Z., Self-powered enzyme-linked microneedle patch for scar-prevention healing of diabetic wounds. *Sci Adv* **2023**, *9* (28), eadh1415.
17. Barman, S. R.; Chan, S. W.; Kao, F. C.; Ho, H. Y.; Khan, I.; Pal, A.; Huang, C. C.; Lin, Z. H., A self-powered multifunctional dressing for active infection prevention and accelerated wound

- healing. *Sci Adv* **2023**, *9* (4), eadc8758.
18. Lumpkin, E. A.; Caterina, M. J., Mechanisms of sensory transduction in the skin. *Nature* **2007**, *445* (7130), 858-65.
 19. Tan, M. H.; Xu, X. H.; Yuan, T. J.; Hou, X.; Wang, J.; Jiang, Z. H.; Peng, L. H., Self-powered smart patch promotes skin nerve regeneration and sensation restoration by delivering biological-electrical signals in program. *Biomaterials* **2022**, *283*, 121413.
 20. Teguh, D. N.; Bol Raap, R.; Koole, A.; Knippenberg, B.; Smit, C.; Oomen, J.; van Hulst, R. A., Hyperbaric oxygen therapy for nonhealing wounds: Treatment results of a single center. *Wound Repair Regen* **2021**, *29* (2), 254-260.
 21. Kim, H. S.; Sun, X.; Lee, J. H.; Kim, H. W.; Fu, X.; Leong, K. W., Advanced drug delivery systems and artificial skin grafts for skin wound healing. *Adv Drug Deliv Rev* **2019**, *146*, 209-239.
 22. Kim, H.; Park, S.; Housler, G.; Marcel, V.; Cross, S.; Izadjoo, M., An Overview of the Efficacy of a Next Generation Electroceutical Wound Care Device. *Military Medicine* **2016**, *181* (5S), 184-190.
 23. Yu, C.; Xu, Z.-X.; Hao, Y.-H.; Gao, Y.-B.; Yao, B.-W.; Zhang, J.; Wang, B.; Hu, Z.-Q.; Peng, R.-Y., A novel microcurrent dressing for wound healing in a rat skin defect model. *Military Medical Research* **2019**, *6* (1).
 24. Dwivedi, C.; Pandey, H.; Pandey, A. C.; Patil, S.; Ramteke, P. W.; Laux, P.; Luch, A.; Singh, A. V., In Vivo Biocompatibility of Electrospun Biodegradable Dual Carrier (Antibiotic + Growth Factor) in a Mouse Model-Implications for Rapid Wound Healing. *Pharmaceutics* **2019**, *11* (4).
 25. Hu, Q.; Wan, X.; Wang, S.; Huang, T.; Zhao, X.; Tang, C.; Zheng, M.; Wang, X.; Li, L., Ultrathin, flexible, and piezoelectric Janus nanofibrous dressing for wound healing. *Science China Materials* **2023**, *66* (8), 3347-3360.
 26. Brown, M. S.; Ashley, B.; Koh, A., Wearable Technology for Chronic Wound Monitoring: Current Dressings, Advancements, and Future Prospects. *Front Bioeng Biotechnol* **2018**, *6*, 47.
 27. Zhao, M.; Song, B.; Pu, J.; Wada, T.; Reid, B.; Tai, G.; Wang, F.; Guo, A.; Walczysko, P.; Gu, Y.; Sasaki, T.; Suzuki, A.; Forrester, J. V.; Bourne, H. R.; Devreotes, P. N.; McCaig, C. D.; Penninger, J. M., Electrical signals control wound healing through phosphatidylinositol-3-OH kinase-gamma and PTEN. *Nature* **2006**, *442* (7101), 457-60.
 28. de Gusmão Correia, M. L.; Volpato, A. M.; Águila, M. B.; Mandarim-de-Lacerda, C. A., Developmental origins of health and disease: experimental and human evidence of fetal programming for metabolic syndrome. *Journal of Human Hypertension* **2011**, *26* (7), 405-419.
 29. Talebi, G. A.; Torkaman, G.; Firoozabadi, M. A.; Mofid, M.; Shariat, S.; Kahrizi, S. J. t. A. I. C. o. t. I. E. i. M.; Society, B., Effects of micro-amperage direct current stimulation on injury potential and its relation to wound surface area in guinea pig. **2007**, 3516-3519.
 30. Jeong, S.-H.; Lee, Y.; Lee, M.-G.; Song, W. J.; Park, J.-U.; Sun, J.-Y., Accelerated wound healing with an ionic patch assisted by a triboelectric nanogenerator. *Nano Energy* **2021**, *79*.
 31. Liang, J.; Zeng, H.; Qiao, L.; Jiang, H.; Ye, Q.; Wang, Z.; Liu, B.; Fan, Z., 3D Printed Piezoelectric Wound Dressing with Dual Piezoelectric Response Models for Scar-Prevention Wound Healing. *ACS Appl Mater Interfaces* **2022**, *14* (27), 30507-30522.
 32. Bouchery, T.; Harris, N., Neutrophil-macrophage cooperation and its impact on tissue repair. *Immunology & Cell Biology* **2019**, *97* (3), 289-298.
 33. Wolcott, L. E.; Wheeler, P. C.; Hardwicke, H.; Rowley, B. A. J. S. m. j., Accelerated healing of skin ulcer by electrotherapy: preliminary clinical results. **1969**, *62* 7, 795-801.

34. Khalil, Z.; Merhi, M. J. T. j. o. g. S. A., Biological sciences; sciences, m., Effects of aging on neurogenic vasodilator responses evoked by transcutaneous electrical nerve stimulation: relevance to wound healing. *2000*, *55* 6, B257-63.
35. Jin, H.-K.; Hwang, T.-Y.; Cho, S.-H., Effect of electrical stimulation on blood flow velocity and vessel size. *Open Medicine* **2017**, *12* (1), 5-11.
36. Davis, S. C.; Ovington, L. G., Electrical Stimulation and Ultrasound in Wound Healing. *Dermatologic Clinics* **1993**, *11* (4), 775-781.
37. Konstantinou, E.; Zagoriti, Z.; Pyriochou, A.; Poulas, K., Microcurrent Stimulation Triggers MAPK Signaling and TGF- β 1 Release in Fibroblast and Osteoblast-Like Cell Lines. *Cells* **2020**, *9* (9).
38. Thawer, H. A.; Houghton, P. E., Effects of electrical stimulation on the histological properties of wounds in diabetic mice. *Wound repair and regeneration : official publication of the Wound Healing Society [and] the European Tissue Repair Society* **2001**, *9* (2), 107-115.
39. Leaper, D. J.; Schultz, G.; Carville, K.; Fletcher, J.; Swanson, T.; Drake, R., Extending the TIME concept: what have we learned in the past 10 years?*. *International Wound Journal* **2012**, *9* (s2), 1-19.
40. Feng, F.; Zhao, Z.; Li, J.; Huang, Y.; Chen, W., Multifunctional dressings for wound exudate management. *Progress in Materials Science* **2024**, *146*.
41. Mani, M. P.; Mohd Faudzi, A. A.; Ramakrishna, S.; Ismail, A. F.; Jaganathan, S. K.; Tucker, N.; Rathanasamy, R., Sustainable electrospun materials with enhanced blood compatibility for wound healing applications—A mini review. *Current Opinion in Biomedical Engineering* **2023**, *27*.
42. Yang, J.; Wang, K.; Yu, D.-G.; Yang, Y.; Bligh, S. W. A.; Williams, G. R., Electrospun Janus nanofibers loaded with a drug and inorganic nanoparticles as an effective antibacterial wound dressing. *Materials Science and Engineering: C* **2020**, *111*.
43. Ma, C.; Hao, S.; Yu, W.; Liu, X.; Wang, Y.; Wang, Y.; Zhao, J.; Zhang, N.; Bai, Y.; Xu, F.; Yang, J., Compliant and breathable electrospun epidermal electrode towards artifact-free electrophysiological monitoring. *Chemical Engineering Journal* **2024**, *490*.
44. Ma, Z.; Huang, Q.; Xu, Q.; Zhuang, Q.; Zhao, X.; Yang, Y.; Qiu, H.; Yang, Z.; Wang, C.; Chai, Y.; Zheng, Z., Permeable superelastic liquid-metal fibre mat enables biocompatible and monolithic stretchable electronics. *Nature Materials* **2021**, *20* (6), 859-868.
45. Zheng, Y.; Li, Y.; Zhao, Y.; Lin, X.; Luo, S.; Wang, Y.; Li, L.; Teng, C.; Wang, X.; Xue, G.; Zhou, D., Ultrathin and highly breathable electronic tattoo for sensing multiple signals imperceptibly on the skin. *Nano Energy* **2023**, *107*.
46. Luo, G.; Liu, J.; Xie, J.; Jing, W.; Li, M.; Zhao, L.; Li, Z.; Yang, P.; Jiang, Z., A highly electrocatalytic, stretchable, and breathable enzyme-free electrochemical patch based on electrospun fibers decorated with platinum nano pine needles for continuous glucose sensing in neutral conditions. *Dalton Transactions* **2023**, *52* (36), 12988-12998.
47. Xu, B.; Li, A.; Wang, R.; Zhang, J.; Ding, Y.; Pan, D.; Shen, Z., Elastic Janus film for Wound Dressings: Unidirectional Biofluid Transport and Effectively Promoting Wound Healing. *Advanced Functional Materials* **2021**, *31* (41).
48. Wang, H.; Duan, W.; Ren, Z.; Li, X.; Ma, W.; Guan, Y.; Liu, F.; Chen, L.; Yan, P.; Hou, X., Engineered Sandwich-Structured Composite Wound Dressings with Unidirectional Drainage and Anti-Adhesion Supporting Accelerated Wound Healing. *Advanced Healthcare Materials* **2022**, *12* (8).
49. Ge, Z.; Guo, W.; Tao, Y.; Sun, H.; Meng, X.; Cao, L.; Zhang, S.; Liu, W.; Akhtar, M.

- L.; Li, Y.; Ren, Y., Wireless and Closed-Loop Smart Dressing for Exudate Management and On-Demand Treatment of Chronic Wounds. *Advanced Materials* **2023**, *35* (47).
50. Wang, Z. Y.; Zhu, Y. J.; Chen, Y. Q.; Yu, H. P.; Xiong, Z. C., Bioinspired Aerogel with Vertically Ordered Channels and Low Water Evaporation Enthalpy for High-Efficiency Salt-Rejecting Solar Seawater Desalination and Wastewater Purification. *Small* **2023**, *19* (19).
51. Mao, J. W.; Han, D. D.; Zhou, H.; Sun, H. B.; Zhang, Y. L., Bioinspired Superhydrophobic Swimming Robots with Embedded Microfluidic Networks and Photothermal Switch for Controllable Marangoni Propulsion. *Advanced Functional Materials* **2022**, *33* (6).
52. Zhang, Y.; Xu, X.; Li, Z.; Xue, Y.; Wang, C.; Li, Q.; Zhao, J.; Wei, N., Design of a bio-inspired nanofiltration channel for self-driven desalination and cleansing. *Desalination* **2024**, *582*.
53. Guo, S.; Liu, X.; Guo, C.; Ning, Y.; Yang, K.; Yu, C.; Liu, K.; Jiang, L., Bioinspired Underwater Superoleophilic Two-Dimensional Surface with Asymmetric Oleophobic Barriers for Unidirectional and Long-Distance Oil Transport. *ACS Applied Materials & Interfaces* **2023**, *15* (18), 22684-22691.
54. Hsu, C.-N.; Mai, N. P. U.; Chen, P.-Y., Effective Unidirectional Wetting of Liquids on Multi-gradient, Bio-inspired Surfaces Fabricated by 3D Printing and Surface Modification. **2024**.
55. Lei, H.; Fan, D., Conductive, adaptive, multifunctional hydrogel combined with electrical stimulation for deep wound repair. *Chemical Engineering Journal* **2021**, *421*.
56. Xie, C.; Li, P.; Han, L.; Wang, Z.; Zhou, T.; Deng, W.; Wang, K.; Lu, X., Electroresponsive and cell-affinitive polydopamine/polypyrrole composite microcapsules with a dual-function of on-demand drug delivery and cell stimulation for electrical therapy. *NPG Asia Materials* **2017**, *9* (3), e358-e358.
57. Marzocchi, M.; Gualandi, I.; Calienni, M.; Zironi, I.; Scavetta, E.; Castellani, G.; Fraboni, B., Physical and Electrochemical Properties of PEDOT:PSS as a Tool for Controlling Cell Growth. *ACS Applied Materials & Interfaces* **2015**, *7* (32), 17993-18003.
58. Simmons, T. J.; Lee, S. H.; Park, T. J.; Hashim, D. P.; Ajayan, P. M.; Linhardt, R. J., Antiseptic single wall carbon nanotube bandages. *Carbon* **2009**, *47* (6), 1561-1564.
59. Jalilinejad, N.; Rabiee, M.; Baheiraei, N.; Ghahremanzadeh, R.; Salarian, R.; Rabiee, N.; Akhavan, O.; Zarrintaj, P.; Hejna, A.; Saeb, M. R.; Zarrabi, A.; Sharifi, E.; Yousefiasl, S.; Zare, E. N., Electrically conductive carbon-based (bio)-nanomaterials for cardiac tissue engineering. *Bioengineering & Translational Medicine* **2022**, *8* (1).
60. Rezvani Ghomi, E.; Niazi, M.; Ramakrishna, S., The evolution of wound dressings: From traditional to smart dressings. *Polymers for Advanced Technologies* **2022**, *34* (2), 520-530.
61. Song, P.; Kuang, S.; Panwar, N.; Yang, G.; Tng, D. J. H.; Tjin, S. C.; Ng, W. J.; Majid, M. B. A.; Zhu, G.; Yong, K. T.; Wang, Z. L., A Self-Powered Implantable Drug-Delivery System Using Biokinetic Energy. *Advanced Materials* **2017**, *29* (11).
62. Xu, G.; Lu, Y.; Cheng, C.; Li, X.; Xu, J.; Liu, Z.; Liu, J.; Liu, G.; Shi, Z.; Chen, Z.; Zhang, F.; Jia, Y.; Xu, D.; Yuan, W.; Cui, Z.; Low, S. S.; Liu, Q., Battery-Free and Wireless Smart Wound Dressing for Wound Infection Monitoring and Electrically Controlled On-Demand Drug Delivery. *Advanced Functional Materials* **2021**, *31* (26).
63. Fu, S.; Yi, S.; Ke, Q.; Liu, K.; Xu, H., A Self-Powered Hydrogel/Nanogenerator System Accelerates Wound Healing by Electricity-Triggered On-Demand Phosphatase and Tensin Homologue (PTEN) Inhibition. *ACS Nano* **2023**, *17* (20), 19652-19666.
64. Zhou, Y.; Jia, X.; Pang, D.; Jiang, S.; Zhu, M.; Lu, G.; Tian, Y.; Wang, C.; Chao, D.;

- Wallace, G., An integrated Mg battery-powered iontophoresis patch for efficient and controllable transdermal drug delivery. *Nature Communications* **2023**, *14* (1).
65. Wu, C.; Jiang, P.; Li, W.; Guo, H.; Wang, J.; Chen, J.; Prausnitz, M. R.; Wang, Z. L., Self - Powered Iontophoretic Transdermal Drug Delivery System Driven and Regulated by Biomechanical Motions. *Advanced Functional Materials* **2019**, *30* (3).
66. Fakhari, A.; Corcoran, M.; Schwarz, A., Thermogelling properties of purified poloxamer 407. *Heliyon* **2017**, *3* (8), e00390.
67. Zhu, Y.; Zhang, J.; Song, J.; Yang, J.; Du, Z.; Zhao, W.; Guo, H.; Wen, C.; Li, Q.; Sui, X. J. A. F. M., A multifunctional pro-healing zwitterionic hydrogel for simultaneous optical monitoring of pH and glucose in diabetic wound treatment. **2020**, *30* (6), 1905493.
68. Yang, J.; Kwon, K. Y.; Kanetkar, S.; Xing, R.; Nithyanandam, P.; Li, Y.; Jung, W.; Gong, W.; Tuman, M.; Shen, Q.; Wang, M.; Ghosh, T.; Chatterjee, K.; Wang, X.; Zhang, D.; Kim, T. i.; Truong, V. K.; Dickey, M. D., Skin-Inspired Capacitive Stress Sensor with Large Dynamic Range via Bilayer Liquid Metal Elastomers. *Advanced Materials Technologies* **2021**, *7* (5).
69. Kireev, D.; Kampfe, J.; Hall, A.; Akinwande, D., Graphene electronic tattoos 2.0 with enhanced performance, breathability and robustness. *npj 2D Materials and Applications* **2022**, *6* (1).
70. Zhang, X.; Chen, G.; Sun, L.; Ye, F.; Shen, X.; Zhao, Y., Claw-inspired microneedle patches with liquid metal encapsulation for accelerating incisional wound healing. *Chemical Engineering Journal* **2021**, *406*.
71. Wang, Z. L., Triboelectric nanogenerators as new energy technology for self-powered systems and as active mechanical and chemical sensors. *ACS Nano* **2013**, *7* (11), 9533-57.
72. Liu, Z.; Li, H.; Shi, B.; Fan, Y.; Wang, Z. L.; Li, Z., Wearable and Implantable Triboelectric Nanogenerators. *Advanced Functional Materials* **2019**, *29* (20).
73. Wang, Z. L., Nanogenerators, self-powered systems, blue energy, piezotronics and piezophotonics – A recall on the original thoughts for coining these fields. *Nano Energy* **2018**, *54*, 477-483.
74. Munirathinam, P.; Anna Mathew, A.; Shanmugasundaram, V.; Vivekananthan, V.; Purusothaman, Y.; Kim, S.-J.; Chandrasekhar, A., A comprehensive review on triboelectric nanogenerators based on Real-Time applications in energy harvesting and Self-Powered sensing. *Materials Science and Engineering: B* **2023**, *297*.
75. Sun, J.; Li, W.; Liu, G.; Li, W.; Chen, M., Triboelectric Nanogenerator Based on Biocompatible Polymer Materials. *The Journal of Physical Chemistry C* **2015**, *119* (17), 9061-9068.
76. Yang, Y.; Xie, L.; Wen, Z.; Chen, C.; Chen, X.; Wei, A.; Cheng, P.; Xie, X.; Sun, X., Coaxial Triboelectric Nanogenerator and Supercapacitor Fiber-Based Self-Charging Power Fabric. *ACS Appl Mater Interfaces* **2018**, *10* (49), 42356-42362.
77. Zhou, C.; Yang, Y.; Sun, N.; Wen, Z.; Cheng, P.; Xie, X.; Shao, H.; Shen, Q.; Chen, X.; Liu, Y.; Wang, Z. L.; Sun, X., Flexible self-charging power units for portable electronics based on folded carbon paper. *Nano Research* **2018**, *11* (8), 4313-4322.
78. Long, Y.; Wei, H.; Li, J.; Yao, G.; Yu, B.; Ni, D.; Gibson, A. L.; Lan, X.; Jiang, Y.; Cai, W.; Wang, X., Effective Wound Healing Enabled by Discrete Alternative Electric Fields from Wearable Nanogenerators. *ACS Nano* **2018**, *12* (12), 12533-12540.
79. Campos-Martin, J. M.; Blanco-Brieva, G.; Fierro, J. L., Hydrogen peroxide synthesis: an outlook beyond the anthraquinone process. *Angew Chem Int Ed Engl* **2006**, *45* (42), 6962-84.
80. Lukes, P.; Appleton, A. T.; Locke, B. R., Hydrogen Peroxide and Ozone Formation in Hybrid

Gas-Liquid Electrical Discharge Reactors. *IEEE Transactions on Industry Applications* **2004**, *40* (1), 60-67.

81. Wang, Y.; Wen, X.; Jia, Y.; Huang, M.; Wang, F.; Zhang, X.; Bai, Y.; Yuan, G.; Wang, Y., Piezo-catalysis for nondestructive tooth whitening. *Nat Commun* **2020**, *11* (1), 1328.

82. Yuan, R.; Yang, N.; Fan, S.; Huang, Y.; You, D.; Wang, J.; Zhang, Q.; Chu, C.; Chen, Z.; Liu, L.; Ge, L., Biomechanical Motion-Activated Endogenous Wound Healing through LBL Self-Powered Nanocomposite Repairer with pH-Responsive Anti-Inflammatory Effect. *Small* **2021**, *17* (50), e2103997.

83. Venkatasubramanian, R.; Siivola, E.; Colpitts, T.; O'Quinn, B., Thin-film thermoelectric devices with high room-temperature figures of merit. *Nature* **2001**, *413* (6856), 597-602.

84. Vu, T. V.; Lavrentyev, A. A.; Gabrelian, B. V.; Kalmykova, K. F.; Vo, D. D.; Tong, H. D.; Hoat, D. M.; Batouche, M.; Luong, H. L.; Khyzhun, O. Y., Effect of DFT methods on electronic structure and K-absorption spectra of InPS4: detailed studies of the optical, thermoelectric and elastic properties. *Materials Research Express* **2019**, *6* (10).

85. Du, S.; Suo, H.; Xie, G.; Lyu, Q.; Mo, M.; Xie, Z.; Zhou, N.; Zhang, L.; Tao, J.; Zhu, J., Self-powered and photothermal electronic skin patches for accelerating wound healing. *Nano Energy* **2022**, *93*.

86. Jang, H. J.; Tiruneh, D. M.; Ryu, H.; Yoon, J. K., Piezoelectric and Triboelectric Nanogenerators for Enhanced Wound Healing. *Biomimetics (Basel)* **2023**, *8* (7).

87. Liu, C.; Peng, M.; Yu, A.; Liu, J.; Song, M.; Zhang, Y.; Zhai, J., Interface engineering on p-CuI/n-ZnO heterojunction for enhancing piezoelectric and piezo-phototronic performance. *Nano Energy* **2016**, *26*, 417-424.

88. Bhang, S. H.; Jang, W. S.; Han, J.; Yoon, J. K.; La, W. G.; Lee, E.; Kim, Y. S.; Shin, J. Y.; Lee, T. J.; Baik, H. K.; Kim, B. S., Zinc Oxide Nanorod-Based Piezoelectric Dermal Patch for Wound Healing. *Advanced Functional Materials* **2016**, *27* (1).

89. Pratihari, S.; Patra, A.; Sasmal, A.; Medda, S. K.; Sen, S., Enhanced dielectric, ferroelectric, energy storage and mechanical energy harvesting performance of ZnO-PVDF composites induced by MWCNTs as an additive third phase. *Soft Matter* **2021**, *17* (37), 8483-8495.

90. Wang, A.; Hu, M.; Zhou, L.; Qiang, X., Self-Powered Well-Aligned P(VDF-TrFE) Piezoelectric Nanofiber Nanogenerator for Modulating an Exact Electrical Stimulation and Enhancing the Proliferation of Preosteoblasts. *Nanomaterials (Basel)* **2019**, *9* (3).

91. Ye, S.; Cheng, C.; Chen, X.; Chen, X.; Shao, J.; Zhang, J.; Hu, H.; Tian, H.; Li, X.; Ma, L.; Jia, W., High-performance piezoelectric nanogenerator based on microstructured P(VDF-TrFE)/BNNTs composite for energy harvesting and radiation protection in space. *Nano Energy* **2019**, *60*, 701-714.

92. Liang, S.; Kang, Y.; Tiraferri, A.; Giannelis, E. P.; Huang, X.; Elimelech, M., Highly hydrophilic polyvinylidene fluoride (PVDF) ultrafiltration membranes via postfabrication grafting of surface-tailored silica nanoparticles. *ACS Appl Mater Interfaces* **2013**, *5* (14), 6694-703.

93. Janmohammadi, M.; Nazemi, Z.; Salehi, A. O. M.; Seyfoori, A.; John, J. V.; Nourbakhsh, M. S.; Akbari, M., Cellulose-based composite scaffolds for bone tissue engineering and localized drug delivery. *Bioactive Materials* **2023**, *20*, 137-163.

94. Han, X.; Chen, L.; Yanilmaz, M.; Lu, X.; Yang, K.; Hu, K.; Liu, Y.; Zhang, X., From nature, requite to nature: Bio-based cellulose and its derivatives for construction of green zinc batteries. *Chemical Engineering Journal* **2023**, *454*.

95. Ghosh, S.; Vaidya, S.; More, N.; Velyutham, R.; Kapusetti, G., Piezoelectric-based bioactive zinc oxide-cellulose acetate electrospun mats for efficient wound healing: an in vitro insight. *Frontiers in Immunology* **2023**, *14*.
96. Cao, Y.; Ren, Q.; Hao, R.; Sun, Z., Innovative strategies to boost photothermal therapy at mild temperature mediated by functional nanomaterials. *Materials & Design* **2022**, *214*.
97. Lukač, M.; Lozar, A.; Perhavec, T.; Bajd, F., Variable heat shock response model for medical laser procedures. *Lasers in Medical Science* **2019**, *34* (6), 1147-1158.
98. Shi, W.; Song, N.; Huang, Y.; He, C.; Zhang, M.; Zhao, W.; Zhao, C., Improved Cooling Performance of Hydrogel Wound Dressings via Integrating Thermal Conductivity and Heat Storage Capacity for Burn Therapy. *Biomacromolecules* **2022**, *23* (3), 889-902.
99. Wang, B.; Pang, M.; Song, Y.; Wang, H.; Qi, P.; Bai, S.; Lei, X.; Wei, S.; Zong, Z.; Lin, S.; Zhang, X.; Cen, X.; Wang, X.; Yang, Y.; Li, Y.; Wang, Y.; Xu, H.; Huang, L.; Tortorella, M.; Cheng, B.; Lee, Y.; Qin, D.; Li, G., Human fetal mesenchymal stem cells secretome promotes scarless diabetic wound healing through heat - shock protein family. *Bioengineering & Translational Medicine* **2022**, *8* (1).
100. Wang, L.; Liu, S.; Wang, Z.; Zhou, Y.; Qin, Y.; Wang, Z. L., Piezotronic Effect Enhanced Photocatalysis in Strained Anisotropic ZnO/TiO₂ Nanoplatelets via Thermal Stress. *ACS Nano* **2016**, *10* (2), 2636-2643.
101. Chen, Y.; Ye, M.; Song, L.; Zhang, J.; Yang, Y.; Luo, S.; Lin, M.; Zhang, Q.; Li, S.; Zhou, Y.; Chen, A.; An, Y.; Huang, W.; Xuan, T.; Gu, Y.; He, H.; Wu, J.; Li, X., Piezoelectric and photothermal dual functional film for enhanced dermal wound regeneration via upregulation of Hsp90 and HIF-1 α . *Applied Materials Today* **2020**, *20*.
102. Liu, Y.; Ai, K.; Liu, J.; Deng, M.; He, Y.; Lu, L., Dopamine-Melanin Colloidal Nanospheres: An Efficient Near-Infrared Photothermal Therapeutic Agent for In Vivo Cancer Therapy. *Advanced Materials* **2012**, *25* (9), 1353-1359.
103. Song, Y.; Wang, C., High-power biofuel cells based on three-dimensional reduced graphene oxide/carbon nanotube micro-arrays. *Microsystems & Nanoengineering* **2019**, *5* (1).
104. Huang, W.; Zulkifli, M. Y. B.; Chai, M.; Lin, R.; Wang, J.; Chen, Y.; Chen, V.; Hou, J., Recent advances in enzymatic biofuel cells enabled by innovative materials and techniques. *Exploration* **2023**, *3* (4).
105. Bati, A. S. R.; Zhong, Y. L.; Burn, P. L.; Nazeeruddin, M. K.; Shaw, P. E.; Batmunkh, M., Next-generation applications for integrated perovskite solar cells. *Communications Materials* **2023**, *4* (1).
106. Lee, J. H.; Jeon, W.-Y.; Kim, H.-H.; Lee, E.-J.; Kim, H.-W., Electrical stimulation by enzymatic biofuel cell to promote proliferation, migration and differentiation of muscle precursor cells. *Biomaterials* **2015**, *53*, 358-369.
107. Kai, H.; Yamauchi, T.; Ogawa, Y.; Tsubota, A.; Magome, T.; Miyake, T.; Yamasaki, K.; Nishizawa, M., Accelerated Wound Healing on Skin by Electrical Stimulation with a Bioelectric Plaster. *Advanced Healthcare Materials* **2017**, *6* (22).
108. Ogawa, Y.; Kato, K.; Miyake, T.; Nagamine, K.; Ofuji, T.; Yoshino, S.; Nishizawa, M., Organic Transdermal Iontophoresis Patch with Built-in Biofuel Cell. *Advanced Healthcare Materials* **2014**, *4* (4), 506-510.
109. Hansen, T. S.; West, K.; Hassager, O.; Larsen, N. B., Highly Stretchable and Conductive Polymer Material Made from Poly(3,4 - ethylenedioxythiophene) and Polyurethane Elastomers.

Advanced Functional Materials **2007**, *17* (16), 3069-3073.

110. Kim, T.-H.; Jeon, W.-Y.; Ji, Y.; Park, E. J.; Yoon, D. S.; Lee, N.-H.; Park, S.-M.; Mandakhbayar, N.; Lee, J.-H.; Lee, H.-H.; Kim, H.-W., Electricity auto-generating skin patch promotes wound healing process by activation of mechanosensitive ion channels. *Biomaterials* **2021**, *275*.

111. Wu, K.; Wu, X.; Chen, M.; Wu, H.; Jiao, Y.; Zhou, C., H₂O₂-responsive smart dressing for visible H₂O₂ monitoring and accelerating wound healing. *Chemical Engineering Journal* **2020**, *387*.

112. Wang, Y.; Wang, X.; Zhou, D.; Xia, X.; Zhou, H.; Wang, Y.; Ke, H., Preparation and Characterization of Polycaprolactone (PCL) Antimicrobial Wound Dressing Loaded with Pomegranate Peel Extract. *ACS Omega* **2023**, *8* (23), 20323-20331.

113. Wang, L.; Su, Q.; Liu, Y.; Yimamumaimaiti, T.; Hu, D.; Zhu, J. J.; Zhang, J. R., A self-powered and drug-free diabetic wound healing patch breaking hyperglycemia and low H₂O₂ limitations and precisely sterilizing driven by electricity. *Chem Sci* **2022**, *13* (41), 12136-12143.

114. Du, S.; Zhou, N.; Xie, G.; Chen, Y.; Suo, H.; Xu, J.; Tao, J.; Zhang, L.; Zhu, J., Surface-engineered triboelectric nanogenerator patches with drug loading and electrical stimulation capabilities: Toward promoting infected wounds healing. *Nano Energy* **2021**, *85*.

115. Yang, Y.; Xu, L.; Jiang, D.; Chen, B. Z.; Luo, R.; Liu, Z.; Qu, X.; Wang, C.; Shan, Y.; Cui, Y.; Zheng, H.; Wang, Z.; Wang, Z. L.; Guo, X. D.; Li, Z., Self-Powered Controllable Transdermal Drug Delivery System. *Advanced Functional Materials* **2021**, *31* (36).

116. Li, J.; Xie, Y.; Zou, X.; Li, Z.; Liu, W.; Liu, G.; Ma, M.; Zheng, Y., Ultrasonic/electrical dual stimulation response nanocomposite bioelectret for controlled precision drug release. *Mater Today Bio* **2023**, *20*, 100665.

117. Tang, W.; Zhu, S.; Jiang, D.; Zhu, L.; Yang, J.; Xiang, N., Channel innovations for inertial microfluidics. *Lab on a Chip* **2020**, *20* (19), 3485-3502.

118. Potgieter, M. D.; Meidany, P., Evaluation of the penetration of nanocrystalline silver through various wound dressing mediums: An in vitro study. *Burns* **2018**, *44* (3), 596-602.

119. Sales, F. C. P.; Ariati, R. M.; Noronha, V. T.; Ribeiro, J. E., Mechanical Characterization of PDMS with Different Mixing Ratios. *Procedia Structural Integrity* **2022**, *37*, 383-388.

120. Bandodkar, A. J.; Lee, S. P.; Huang, I.; Li, W.; Wang, S.; Su, C. J.; Jeang, W. J.; Hang, T.; Mehta, S.; Nyberg, N.; Gutruf, P.; Choi, J.; Koo, J.; Reeder, J. T.; Tseng, R.; Ghaffari, R.; Rogers, J. A., Sweat-activated biocompatible batteries for epidermal electronic and microfluidic systems. *Nature Electronics* **2020**, *3* (9), 554-562.